NASA-TM-20250003000

# Ground-Based RFI Mitigation Approaches for UAS Flight Operations in Urban Environment

*Kaveh Darafsheh, Anne I. Mackenzie, Truong X. Nguyen, Cuong C. Quach, Yamira Santiago-Espada, and Kyle M. Smalling*

*Langley Research Center, Hampton, Virginia*

*Christoper M. Morris and Andrew T. Turner*

*Analytical Mechanics Associates of Hampton, Virginia*

April 2025

# NASA STI Program Report Series

Since its founding, NASA has been dedicated to the advancement of aeronautics and space science. The NASA scientific and technical information (STI) program plays a key part in helping NASA maintain this important role.

The NASA STI program operates under the auspices of the Agency Chief Information Officer. It collects, organizes, provides for archiving, and disseminates NASA's STI. The NASA STI program provides access to the NTRS Registered and its public interface, the NASA Technical Reports Server, thus providing one of the largest collections of aeronautical and space science STI in the world. Results are published in both non-NASA channels and by NASA in the NASA STI Report Series, which includes the following report types:

- TECHNICAL PUBLICATION. Reports of completed research or a major significant phase of research that present the results of NASA Programs and include extensive data or theoretical analysis. Includes compilations of significant scientific and technical data and information deemed to be of continuing reference value. NASA counterpart of peer-reviewed formal professional papers but has less stringent limitations on manuscript length and extent of graphic presentations.

- TECHNICAL MEMORANDUM. Scientific and technical findings that are preliminary or of specialized interest, e.g., quick release reports, working papers, and bibliographies that contain minimal annotation. Does not contain extensive analysis.

- CONTRACTOR REPORT. Scientific and technical findings by NASA-sponsored contractors and grantees.

- CONFERENCE PUBLICATION. Collected papers from scientific and technical conferences, symposia, seminars, or other meetings sponsored or co-sponsored by NASA.

- SPECIAL PUBLICATION. Scientific, technical, or historical information from NASA programs, projects, and missions, often concerned with subjects having substantial public interest.

- TECHNICAL TRANSLATION. English-language translations of foreign scientific and technical material pertinent to NASA's mission.

Specialized services also include organizing and publishing research results, distributing specialized research announcements and feeds, providing information desk and personal search support, and enabling data exchange services.

For more information about the NASA STI program, see the following:

- Access the NASA STI program home page at http://www.sti.nasa.gov

- Help desk contact information:

https://www.sti.nasa.gov/sti-contact-form/
and select the "General" help request type.

NASA-TM-20250003000

# Ground-Based RFI Mitigation Approaches for UAS Flight Operations in Urban Environment

*Kaveh Darafsheh, Anne I. Mackenzie, Truong X. Nguyen, Cuong C. Quach, Yamira Santiago-Espada, and Kyle M. Smalling*

*Langley Research Center, Hampton, Virginia*

*Christopher M. Morris and Andrew T. Turner*

*Analytical Mechanics Associates of Hampton, Virginia*

National Aeronautics and
Space Administration

Langley Research Center
Hampton, Virginia 23681-2199

April 2025

# Acknowledgements

The authors would like to thank NASA's Aeronautics Research Mission Directorate for its leadership, support, and sponsorship regarding the subject of this report. In particular, the Program and Project Managers, Akbar Sultan, John Koelling, Misty Davies, and Kyle Ellis. Without their support, outside-the-box thinking, and constructive critiques, the concept exploration leading to this report would not have been possible. Special thanks to Safety Critical Avionics Systems Branch Managers Eric Cooper and Roger Bailey for support getting physical access to research facilities during COVID restrictions.

Very special thanks to Steve Young, the Sub-Project Manager of Emerging Operations Technical Challenge for supporting the work and generous insight and helpful discussions which set the direction of the work and guiding the team along the way with insight and energy. And thanks to Ken Dudley and Jay Ely for technical insight and evaluation of spectrum monitoring systems and establishing technically feasible objectives. Special thanks to Langley's Accelerating Collaboration & Technologies to Architect a Cultural Transformation (ACT2) Portfolio Manager, Patricia Glaab, for supporting installation of the spectrum monitoring system at Langley Research Center flight operations range.

Key contributors to the R&D and testing were Kevin Barnes, Scott Dorsey, Mike Scherner, Laura Smith, Sixto Vazquez, and Haylee Winters. Thank you all for your dedication, creativity, and can-do spirit.

# Table of Contents

# List of Figures

## List of Tables

## List of Acronyms

AC .............. advisory circular
ACT2 ........... Accelerating Collaboration & Technologies to Architect a Cultural Transformation
AGC ............ automatic gain control
AGL ............. above ground level
ALDF ........... Aircraft Landing Dynamics Facility
AOSP........... Airspace Operations and Safety Program
ARMD ......... Aeronautics Research Mission Directorate
ARP ............. aerospace recommended practice
ASSURE ....... The Alliance for System Safety of UAS Through Research Excellence
BP ................ battery prognostics
BER ............ bit error rate
BVR ............ beyond visual range
BVLOS ......... beyond visual line of sight
C2 ................ command and control
CEM ............ computational electromagnetic modeling
CERTAIN I ... City Environment for Range Testing of Autonomous Integrated Navigation, Area I
DO................ RTCA document
EMI ............. electromagnetic interference
FAA ............. Federal Aviation Administration
FCC ............. Federal Communications Commission
FIMS ........... Flight Information Management System
FTDMA ....... frequency and time domain multiple access
GPS ............. Global Positioning System
HIRF ............ high-intensity radiation facility, high-intensity radiated fields
IASMS ......... In-Time Aviation Safety Management System
IoT .............. Internet of things
I/Q .............. in-phase and quadrature
ISO .............. International Organization for Standardization
ITU .............. International Telecommunication Union
JSON ........... JavaScript Object Notation
LaRC ........... Langley Research Center
LOS ............. line of sight
NASA ......... National Aeronautics and Space Administration
NAVQ .......... navigation quality
NPCRA ........ nonparticipant casualty risk assessment
OS&N........... observation, sensing, and networks
OSI ............... open systems interconnection
PAV ............ personal air vehicle
PER ............. package error rate
PLI ............... power line interference
PtT ............... proximity to threat
REM ........... radio frequency environment map
RF ............... radio frequency

RFC ………… request for comments
RFI ………….. radio frequency interference
RFID ……….. radio frequency identification
RTCA ……….. Radio Technical Committee for Aeronautics
SAE ………….. Society of Automotive Engineers
SDSP ……….. supplemental data service provider
SFCs ………… services, functions, and capabilities
SIR ………….. signal-to-interference ratio
SNR ………… signal-to-noise ratio
SO ……………. spectrum occupancy
SWS ……….. System-Wide Safety Project
TCP/IP ……… Transmission Control Protocol/Internet Protocol
TDOA ………. time difference of arrival
UAS ………… uncrewed aircraft system
URL ………….. uniform resource locator
UTM …………Universal Transverse Mercator
VSG ………… vector signal generator
WLAN ……… wireless local area network
XML ………… extensible markup language

## Abstract

*As civilian drone use matures and urban air taxi vehicle development nears approval, the ability to operate these two classes of vehicles allows operators to offer an array of marketable use cases in many urban economies. However, it is known from prior research that radio frequency interference (RFI) can present real safety threats to these operations, and hence, needs to be addressed to facilitate safe drone operations in urban environments. NASA'S System-Wide Safety Project, Technical Challenge 2 has created an interactive RF Service to help UAS operators mitigate RF hazards by avoiding flight areas where RFI would be encountered. Five concepts are presented, utilizing ground-based real-time and historical measurements, FCC data, and electromagnetic modeling based on ray tracing. Based on real-time detected or previously known radiating sources, radiated power levels are calculated for altitudes or trajectories where flights are planned. Expected signal power levels, signal-to interference ratios (SIR), and spectrum occupancy (SO) are displayed as 2-D graphics. Areas of expected RFI hazard are displayed based on user input of hazard-related thresholds.*



## Introduction: The In-Time Aviation Safety Management System (IASMS) Concept

To facilitate safe air taxi and drone operations in low altitude urban centers, NASA is developing technologies to help operators address the complex RF environment and the safety hazards attendant to these operations. This research is performed by the System-Wide Safety (SWS) Project within the Airspace Operations Safety Program (AOSP) portfolio under NASA's Aeronautics Research Mission Directorate (ARMD). The SWS Project proposes using an In-Time Aviation Safety Management System (IASMS) to help operators mitigate hazards during various phases of flight operations [1, 2]. The concept for the IASMS deploys several services, functions, and capabilities (SFCs) which, together, help to monitor, assess, and mitigate safety hazards. As described in [1], these SFCs may be deployed in the aircraft, on the ground station, or as on-demand cloud services. Figure 1, repeated from [1], illustrates a test architecture instantiated at NASA for developmental testing of SFCs in the IASMS concept.

This report describes the development of a part of the IASMS, the Radio Frequency Interference (RFI) Service, an on-demand cloud service that helps mitigate RFI in urban operations environments (yellow oval in figure 1). This service incorporates several workflows that produce information for operators to use in mitigating RFI during flight planning and pre-flight activities. The RFI Service interfaces with Observation, Sensing, and Networks (OS&N) to obtain or compute the RFI information to report to the operator who, in turn, uses flight planning or ground station tools to interact with the RFI Service.

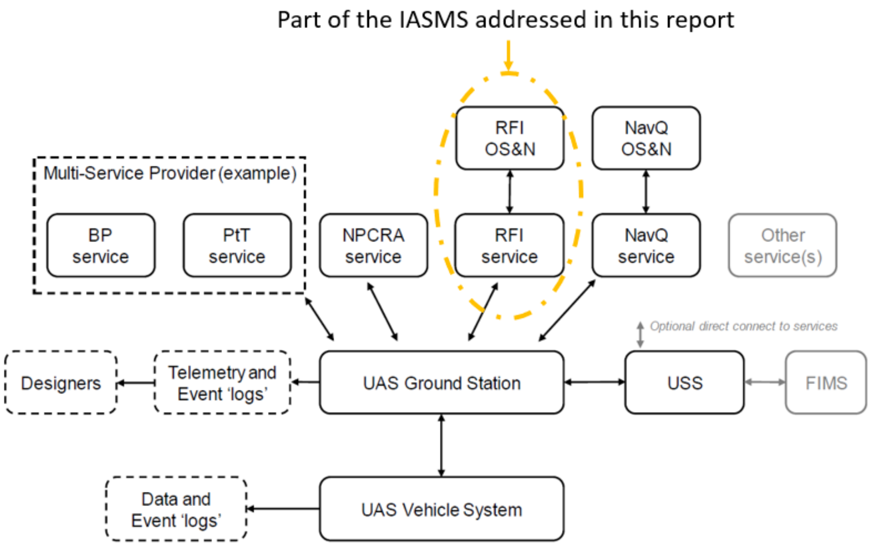


Figure 1. IASMS concept and test architecture repeated from [1] showing the focus area for this report.

An important objective of the IASMS is to present timely, intuitive safety metrics that enable operators or on-board autonomous algorithms to employ effective mitigations for a host of hazards. The RFI Service provides RF spectrum power and frequency information for operators during flight planning to avoid plotting a flight path into known RFI hazard areas. In this report, several concepts and workflows are described at varying stages of deployment. The RFI Service fuses information from sensors monitoring the flying environment with models and databases to create map and indicator products. The safety metrics are derived by combining these products with knowledge of the planned flight path and the vehicle's RF sensitivity and tolerances. More specifically, the map products give the levels or other RF characteristics of the flying environment, while the vehicle information provides the tolerance thresholds at which those levels become problematic for the flight operation**.** The approaches considered here are:

- Calculation of radiated power at specific frequencies at the flight altitude using known detected sources.
- Calculation of link power budget along the planned flight path.
- Data mining FCC or other published records of known transmitters in the region of a planned flight, followed by calculation of radiated power at specific frequencies at the flight altitude or along the planned flight path.
- Calculation of spectrum occupancy in the frequency band of interest due to measured RF sources in the region of a planned flight.
- Use of historical data to project what the RF environment would be during the flight period.

During planning and preflight, the RFI Service communicates with flight planning or ground station tools to obtain specific information about flight paths and vehicle tolerances to determine if RFI hazards will be encountered along the flight path. Specific information needed from the operator to create the hazard decision information is discussed in the service descriptions.

This paper starts with a brief study of the classification of various types of RFI, then describes the safety metrics and mitigation approaches researched under the auspices of the SWS/TC2 sub-project.

## Background

RFI is a known hazard for manned and unmanned air vehicles operating in the vicinity of airports and urban centers. Li et al. performed assessment of front-door and back-door RFI impact on drone operations [3] and later performed risk analysis of RFI in [4] along with flight measurements. Existing standards such as SAE ARP 5583A [5], RTCA DO-160 [6], and FAA regulations [7, 8] govern minimum RF exposure tolerance and testing of avionics for manned vehicles in these environments. Due to reduced size, weight and power margins for these systems, imposing transport standards on uncrewed aircraft systems (UAS) severely reduces their economic viability by reducing their range because of the extra weight added to meet avionics shielding requirements. Also, added testing prolongs the UAS and air taxi vehicle development timeline and delays operational approval.

Radio frequency interference impacts safe operation of drones and personal air vehicles (PAV) in primarily two ways. The first way RFI hazards occur is when the drone and PAV transit in the vicinity of high RF energy. During these transit segments, the fortuitous combination of frequency, field level, and other coupling factors can induce errant signals in electronic wiring or sensor components. Depending on the coupling path and the components impacted, this type of RFI hazard may manifest as data or sensor errors, intermittent faults, or permanent failures in different components of the vehicle avionics systems. These often untraceable upsets erode the operator's confidence in the vehicle and create other hazards when the damage from the RF coupling is more extensive or permanent.

The second way RFI hazards impact safe operations along the flight path is when the drone or PAV encounters intentional (legal or otherwise) or unintentional transmissions in the frequency range used by on-board communication equipment. The interference problem is amplified by the use of spread spectrum devices, for example those used for UAV command and control. These devices require wide receiver bandwidths, which increase detected noise power as well as receiver noise power, compared to narrowband devices. The interfering transmissions reduce the comparative strength of the intended signal and degrade the ability of the on-board communication equipment to communicate with the intended ground systems. In the worst case, this can result in lost link scenarios, precipitating loss of situation awareness for ground operators and other hazards.

A survey of various classifications of RFI is given in the next section to provide context for the later safety metrics discussions. The RFI safety metrics are then identified along with general approaches for RFI hazard mitigation. Specifics about the RF products along with the safety metrics and RF hazards they address are separately described under model-based approaches, measurement approaches, and database approach sections. Some detail is also given on how the information may be presented at the ground station or to on-board systems to facilitate use of the information.

## The Radio Frequency Interference (RFI) Hazard

### The Urban RF Environment

The urban radio frequency environment refers to the electromagnetic spectrum within urban areas. This spectrum is characterized by the presence of numerous RF signals originating from various sources. It encompasses the radio waves and signals used for communication, broadcasting, wireless technology, and other wireless applications. The RF environment in urban areas is complex and diverse, influenced by factors such as population density, infrastructure, building structures, and the presence of numerous electronic devices.

The urban RF environment can be highly congested due to the overlapping of multiple signals sharing the same space and frequency bands and the presence of obstacles like buildings, which can cause signal reflections, interference, and signal attenuation. These factors pose challenges for signal propagation and require careful planning and optimization of communication networks to ensure reliable and efficient communication in urban areas.

In an urban RF environment, one can find a wide range of RF signals and frequencies being utilized. These include cellular networks, including 2G, 3G, 4G, and 5G; wireless local area networks (WLANs) from homes and businesses; broadcast services from terrestrial radio and television; public safety communications; microwave links for point-to-point communication; satellite communication with highly directional antennas; and signals from portable devices including wireless phones, Bluetooth devices, RFID, and the Internet of Things (IoT).

### Types of Interference: Environmental Hazards

RF environmental hazards to an air vehicle can come in various forms. These hazards are associated with the aircraft's external environment. One form of interference is termed high-intensity radiated fields, or HIRF. HIRF interference comes from strong external emitters that couple energy onto the vehicle's wiring and electronics, which can cause undesirable effects simultaneously on multiple vehicle systems. HIRF transmitters include broadcast transmitters, radar, point-to-point links, and other wireless communication technologies. They tend to be in fixed locations; however, they can also be mobile such as radars on ships and aircraft. Other interfering sources are transmitters using the same frequencies or frequencies nearby those which the aircraft receivers are designed to receive.

RF environmental hazards can disrupt or degrade radio frequency communication and navigation signals, leading to communication/navigation issues and performance degradation. Some common types of environmental RF interference hazards include:

- Radio Frequency Interference (RFI): RFI refers to interference caused by signals from different transmitters overlapping or when unwanted signals disrupt the desired communication. Subsets of RFI are co-channel interference when multiple transmitters use the same frequency or channel, and adjacent channel interference when the signals of neighboring channels overlap or interfere with each other.
- Electromagnetic Interference (EMI): EMI occurs when electromagnetic signals from one device or source interfere with the signals of another device. This interference can be caused by devices that emit unintentional electromagnetic radiation such as faulty electrical equipment, faulty wiring, electronic devices with inadequate shielding, and improper operation of RF devices.
- Intermodulation Interference: Intermodulation interference occurs when multiple signals with different frequencies interact nonlinearly, creating additional signals at frequencies that were not present initially. These unwanted signals can interfere if created in the vehicle's communication bands.
- Atmospheric Interference: Atmospheric conditions, such as thunderstorms, solar activity, lightning, and other atmospheric disturbances, can introduce interference in the RF spectrum.

- Jamming: Intentional interference, known as jamming, involves the deliberate transmission of strong RF signals to disrupt or block communication in a specific frequency band or channel. Jamming can be a security threat in sensitive areas.
- Power Line Interference (PLI): Power Line Interference is caused by the presence of electrical power lines and equipment. These power lines can emit electromagnetic noise that interferes with nearby radio frequency signals.

These RF interference hazards can affect various onboard electronics and communication systems. Identifying and mitigating these interference sources are crucial for ensuring reliable and efficient communication in the RF environment.

### Frequencies of Concern for Link Continuity

RFI can disrupt and cause loss of communication links to and from the vehicles, potentially creating hazardous situations that may even result in the loss of vehicles. Minimizing RFI through spectrum management and interference avoidance can lead to more robust communication links. RFI is most likely to occur when vehicles operate in a crowded environment with similar vehicles sharing the space and spectrum. Some of the frequencies of concern are:

- 433 MHz, 915 MHz, 1.2 GHz, 1.3 GHz, 2.4 GHz, 5.8 GHz: Command and control (C2) signals for line-of-sight (LOS) operation
- 700 MHz and 1700-2100 MHz 4G cellular frequencies: C2 for beyond-visual-line-of-sight (BVLOS) operation
- L, K, and Ka-band satcom frequencies: C2 for BVLOS operation
- 1227.6 MHz, 1575.42 MHz: GPS satellite signals
- 5030-5091 MHz: Available for non-networked operations using dynamic frequency allocation under new FCC rules [9]
- 27 MHz, 72 MHz, 400 MHz, 433 MHz, 900-915 MHz, 1.2 GHz, 1.3 GHz, 2.4 GHz, 5.8 GHz: Data telemetry

## RFI Mitigation

RFI by nature is primarily frequency, power, and location dependent. The actual occurrence of RFI secondarily depends on temporal, incident geometry, and shielding effectiveness factors. The difficulty of identifying where and when RFI events occur stems from finding the coincidence of all six of these factors. However, RFI mitigation can be successful just by avoiding the primary three conditions – frequency, power, and location. If the primary factors do not occur, the secondary factors are inconsequential and RFI hazard can be avoided.

The concepts for RFI mitigation in this work center around providing tailored information so operators can ensure their flight paths avoid locations containing the frequency and power content to which the vehicle is sensitive. Tailoring is achieved using information services to interact with operator tools. As figure 2 illustrates, the operator would use this service during planning to send vehicle and mission specifics to the service and the service would respond with tailored information products to aid in avoiding HIRF or link issues.

Researchers deployed an information service at NASA Langley to develop and test several approaches for producing RFI mitigation products and interacting with several software applications used by operators. Both measurement and modeling-based approaches were researched to build workflows for assessing the RF conditions in the flight environment. The test area for this work is Langley's CERTAIN I Flight Test Range. The services have access to RF monitors deployed in the CERTAIN I Range to feed spectrum and other measurements into the workflows.

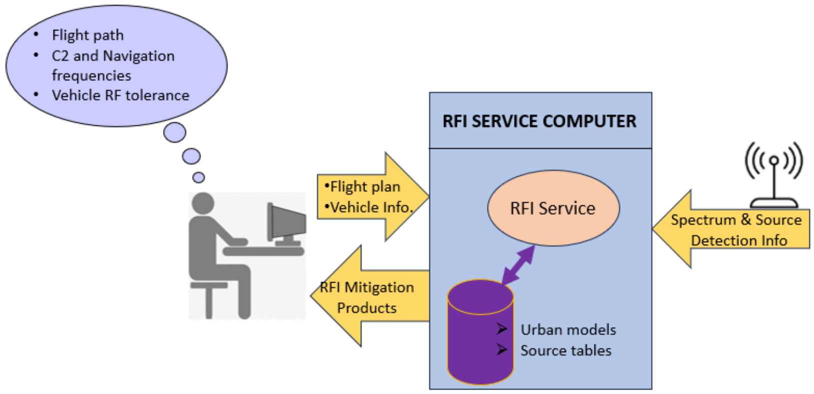


Figure 2. RFI Service user planning a flight. Multiple RFI mitigation products cater to UAS operator needs.

The goal of the effort is to use novel approaches to create information products to assist operators in avoiding RFI hazards during flight planning.

## The Radio Frequency Measurement System

RF monitoring is accomplished using a specialized network of distributed sensors nodes from CRFS™ Inc. [10]. There are currently five such nodes in the measurement network installed in the CERTAIN I range as illustrated in figures 3 and 4. The system is capable of spectrum recording, interference identification, security monitoring, and other spectrum monitoring and management functions. The system comes with server software to facilitate automated processes and is ideally suited for this RFI Service development work.

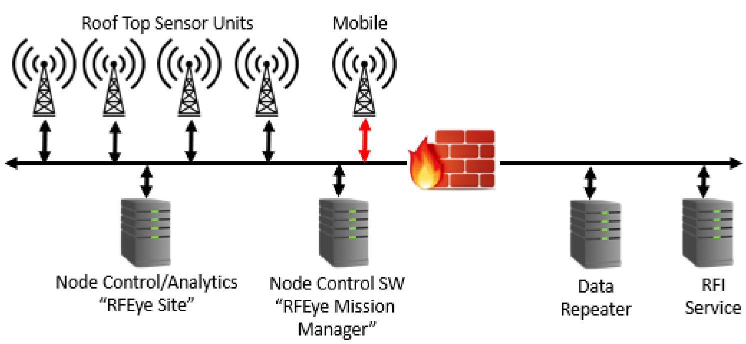


Figure 3. Network configuration for CRFS and RFI systems.

The network uses synchronized measurements of distributed sensors to determine the signal strength and 2-D location of RF transmitters based on the differences in arrival times of the transmitted signals (TDOA location). The receivers are strategically placed to encircle the geolocation coverage area. These time differences, combined with the known positions of the receivers, are used to determine by triangulation the location of the transmitters. The system is also capable of tracking, spectrum recording and management, interference identification, security monitoring, and several other functions.

Each node is capable of measurement from 10 MHz to 8 GHz, with up to 100 MHz instantaneous bandwidth. Two switchable, vertically polarized omnidirectional antennas are used. A dipole antenna (Steatite QOM-SL-0.01-1-N-SG-R, 10 MHz – 1 GHz) is used for frequencies below 1 GHz, and a "lantern" antenna (Steatite QOM-SL-0.8-40-K-SG-L, 0.8 GHz – 40 GHz) for frequencies above 1 GHz. Real-time recording of I/Q data for further analysis is also possible. The node, model CRFS RFeye 100-8, has a typical noise figure of 6-10 dB at the maximum sensitivity.

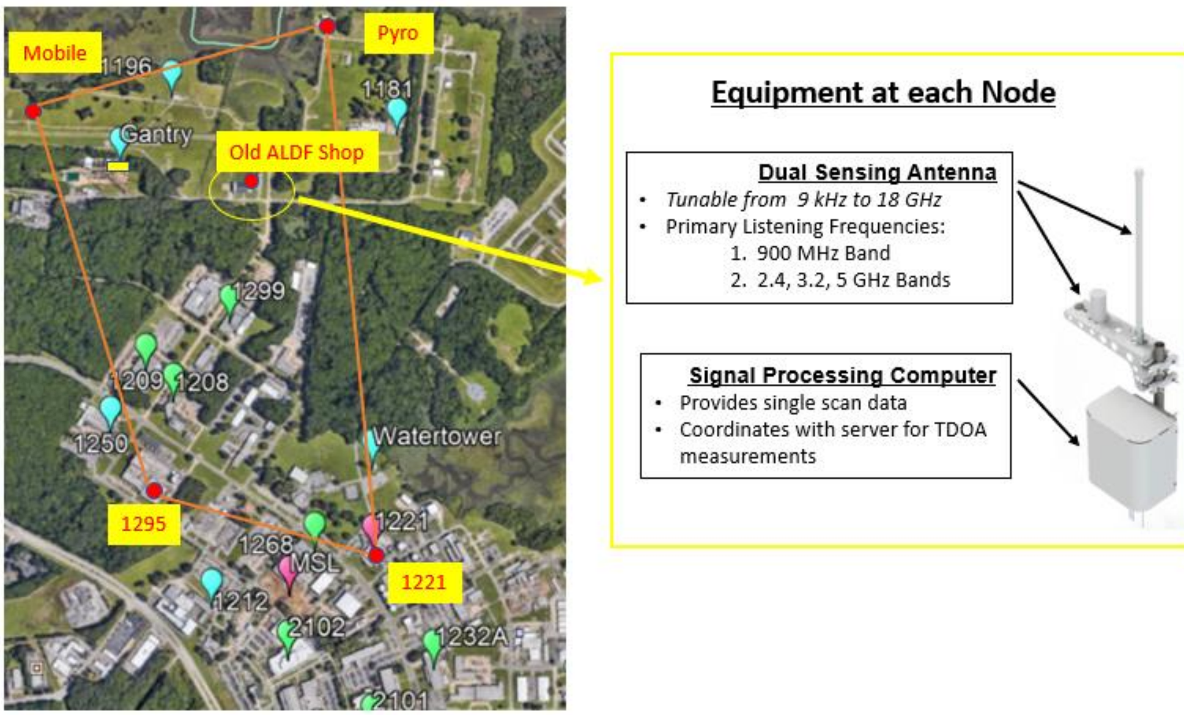


Figure 4. Networked RF monitor system by CRFS™. Red dots indicate locations of CRFS Nodes. Other color balloons indicate location of weather and other sensors used for flight operations. Photo underlay from Google Maps™

The nodes can be set to monitor spectrum in designated frequencies. The spectrum measurement data can also be queried directly from the node for live monitoring and recording without a need for the proprietary software. Several of the nodes were used for spectrum recording and occupancy computation in this study. Using a CRFS software tool (RFeye Mission Manager ™), the chosen receivers were set to periodically record the spectrum data in the frequency bands of interest, and the received RF power data were then exported for analysis.

## RFI Service – Implementation

Table 1 lists the workflows associated with five RFI mitigation approaches in various stages of implementation and testing in the LaRC RFI mitigations service. The table gives cursory characteristics of the workflows, which are discussed in later sections. Workflows 1 and 2, which are used to address HIRF and link health hazards, are model-based approaches augmented with measurements for source detection. Measurement-based approaches are discussed in workflows 3 and 4. These take advantage of the RF monitor system installed in CERTAIN I to also address HIRF and link continuity hazards. Finally, workflow 5 uses data mining to address the HIRF hazard with some consideration to minimize vehicle-specific data. Strengths and weaknesses of each approach are discussed in the workflow descriptions. Implementation and display details are given, where the development is a bit more mature.

Table 1. Summary of RFI service workflows

| Workflow | Title | RFI Hazard Addressed | Flight Phase |
|---|---|---|---|
| 1 | RF Environment Maps | HIRF | Flight Planning, Pre-Flight |
| 2 | Link Continuity Hazards Mitigation using Modeling. | Link Loss | Flight Planning, Pre-Flight |
| 3 | Spectrum Occupancy | Link Loss | Pre-Flight, in-flight |
| 4 | Diurnal levels (Field levels by the hour) | HIRF | Pre-Flight |
| 5 | Stay-out Regions | HIRF | Flight Planning, Pre-Flight |

The workflows calculate metrics for various RF characteristics in the flying environment. These metrics do not by themselves reveal hazardous conditions until the flight path and the vehicle tolerances are defined. The flight path is defined by the operator during flight planning to accomplish the desired mission. The vehicle selected for the mission determines the RF hazard thresholds. The specific tolerance parameters needed by the service depend on the hazards that the operator wishes to address. Determining HIRF or link loss hazards for flight generally requires vehicle RF information such as 1) in-band receiver sensitivity, 2) bandwidth tolerance of the communication protocol, and 3) out-of-band RF exposure limits at which on-board equipage can still properly function.

In the ideal case, as the drone industry matures, this information would be provided by the drone manufacturer. The in-band information is often available with the technical information of the communication equipage installed on the vehicle. The out-of-band information may require HIRF exposure measurements much like what is performed by FAA's Center of Excellence for UAS Research [11]. Absent the vehicle testing, qualitative assessments from domain experts reviewing the installation of on-board electronics might be minimally useful. The vehicle information is crucial in this mitigation approach as it sets the decision points for triggering mitigation actions. And because susceptibility and minimum communication signal levels vary based on vehicle configuration and communication hardware used, these thresholds are necessarily vehicle-specific. Having the information come from the operator also allows the operator to specify additional margins above the manufacturer's thresholds to account for the risk profile the operation is willing to accept.

### Workflow 1: Avoiding RFI by Using RF Environment Maps (REMs) During Flight Planning

RF environment mapping (REM) is a technique commonly used to assess the spectrum environment. This is often done by driving around an area of interest with a vehicle equipped to survey the spectrum environment and geolocate frequency and field strength data. This data is often used to determine signal strength for urban communication systems. A slight variation is to survey transmission towers - ironically with drones [12, 13]. Tower surveys are periodically needed by owners to obtain required verification data to show certificating authorities that the transmitting tower is radiating the correct power levels in the correct direction.

REMs provide awareness of the RF frequency and power content in the flight environment. SWS researchers studied the use of REMs for HIRF hazard mitigation by applying them in the same way that weather maps are used for aviation safety. One key is to produce REMs at resolutions applicable for urban flight; another is to make the information searchable in the geographic context so that RF characteristics of the environment can be identified relative to the vehicle's flight path. Thresholding this data to the vehicle's tolerance specifications allows operators to identify whether the flight path takes the vehicle into geographic regions that exceed the vehicle's HIRF tolerance. This can then be displayed in various intuitive ways to assist operators in identifying the flight segments that may encounter RFI hazards and altering the flight path to avoid those hazards.

The REM workflow can best be summarized in two parts: 1) creating the REMs and 2) deploying the searchable service. REM creation encompasses creating an environment model, using simulation tools, and parceling the resulting information based on combining RF and flight operations characteristics. Deployment covers the data marshalling, client information exchange, and display concept to help drone and PAV operators use the information.

### *Creating REMs with Computational Electromagnetic Modeling and Simulation*

REM creation is governed by the selected computational electromagnetic (CEM) simulation tools. Several tools are available on the market which use various approaches for computing REM. WinProp™ is the CEM simulation software used in this work to compute REMs. WinProp™ is a subset of the ALTAIR Hyperworks™ tool suite that predicts radiation levels encountered at a selected frequency and location. It geolocates the frequency and power levels in 2-D elevation maps given a 3-D model of the operating area. Figure 5 gives the information consolidated and fed to WinProp™ to calculate REMs.

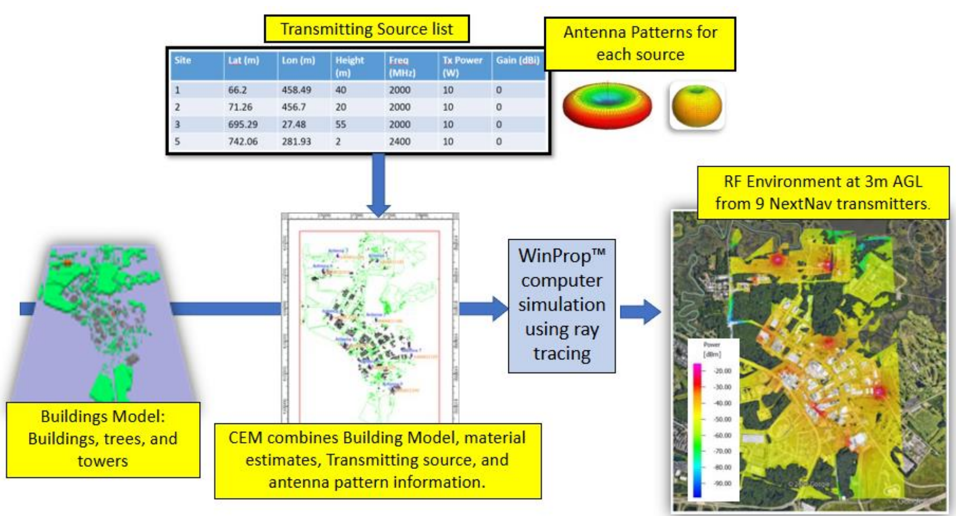


Figure 5. Input data used by WinProp ™ to create an REM. Map underlay from Google Maps™

The models combine information about transmitting sources, 3-D descriptions of structures in the flying environment, and electrical characteristics of those structures. The transmitter information includes location of transmitter, radiating power and antenna pattern. The 3-D model includes geometry descriptions of structures such as buildings and trees. Ideally, anything in the flying space that is of consequence to the RF environment should be included. Electrical properties at the frequency of interest are assigned to each object in the outdoor database model. These properties include transmission, reflection, diffraction, and scattering losses. Separate models are created for each frequency band of interest. The 3-D model provides information for the CEM tool to compute REMs.

Several ways were examined to derive information about transmitting sources. As seen in figure 5, the location, frequency, power, and antenna pattern for each radiating source are input to the CEM simulation. Initial work started with a static list of transmitters known to be installed in the CERTAIN I range. Another option for improving the source list is to search FCC records of transmitters which operate in the flying area, or more importantly, project RF energy into the area. Researchers also studied ways to use an RF measurement system to generate and maintain a list of detected transmitters. The RF measurement system detects RF transmissions using the Time Difference of Arrival (TDOA) method to triangulate approximate positions of the sources.

3-D models representing the CERTAIN I operating range and other areas were created for test and development. Several methods were used to create 3-D building models. The most tedious method was to create shapefiles from lidar scans of the flying area. A simpler approach is to purchase them from commercial sources. Additionally, many municipalities also have this data from other municipal functions. Examples of CEM models of Langley Research Center (LaRC) and a section of the City of Hampton are shown in figure 6. Fundamentally, signals of different frequencies may coexist in the same environment with very minimal or no interaction. Also, EM properties can vary in the same material at different frequencies. These circumstances necessitate performing a separate simulation for each frequency band of interest. Each model can then be used to compute REMs for all altitudes of concern for the frequency.

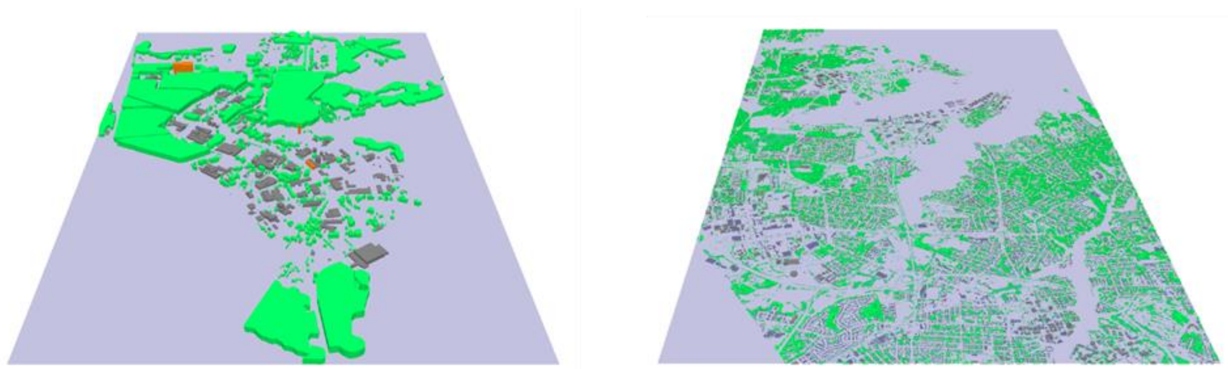

Figure 6. 3-D models of Langley Research Center (left) and a section of the City of Hampton (right).

Ray tracing is used to compute radiation intensity at a particular altitude over a large area. Rays are cast from each transmitting source and the RF energy is collected in dBm assuming an isotropic receiving antenna. At the time of this work, WinProp™ generates REMS for each of the transmitting sources in series, and the various results are added in post processing to provide one multisource REM. Figure 7 shows an example of the resulting multi-source REM without the buildings model overlay. In this example, the power calculation is done at 100 m AGL for nine NextNav™ transmitters installed at LaRC.

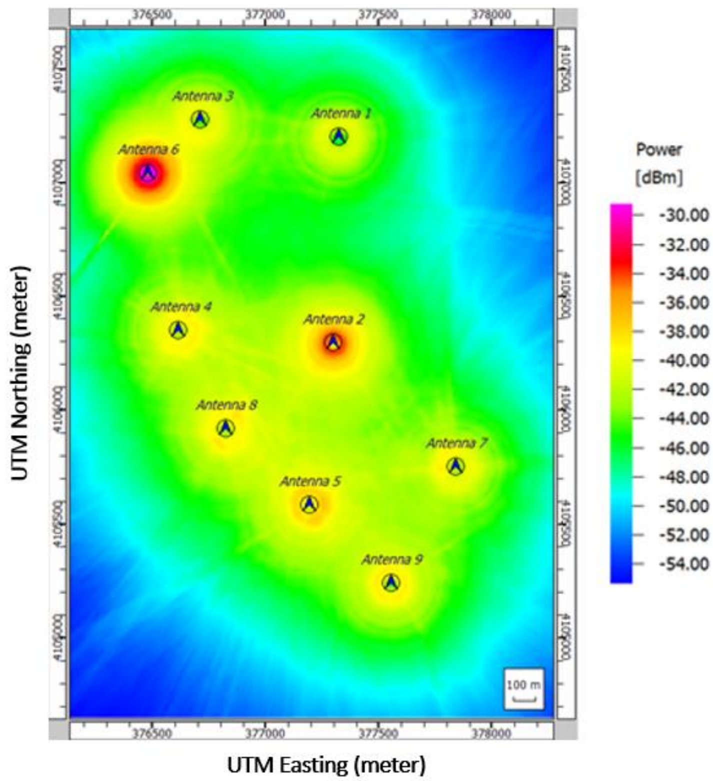


Figure 7. REM showing radiated power at 100 m AGL from NextNav™ antennas at LaRC.

### *Creating REMs for Multiple Elevations*

After the 3-D models are created for input to the CEM tool, the process of generating the REM can be time consuming depending on the size of the flying space and the number of objects (buildings, trees, …) in the model. To provide reasonable service response, a preprocessed outdoor database model is implemented for specific altitudes or for defined points along the flight path only. As earlier mentioned, the CEM tool can create REMs at specific elevations for specific frequencies. The selection of frequencies and altitudes for preprocessed models takes into consideration what frequencies are detected or known to be radiating in the flying area and what altitudes are common for vehicle operations. It is important to have REMs at multiple altitudes for each frequency. In urban environments, REMs at lower elevations can be substantially different from those at higher elevations even for the same transmitter. This is because, at lower elevations, there often are more terrestrial features and buildings to create a multipath environment.

In the case of the CERTAIN I range, a number of 900 and 2400 MHz transmitters are known to be in use. Accordingly, researchers created a preprocessed outdoor database model for each frequency and altitude of interest. Each REM contains the RF energy contribution from all sources at a given frequency and at the selected altitude. Typical altitudes for drone operations at the CERTAIN I range were selected.

### *Model Verification Measurements*

In order to verify the simulation results at Langley Research Center, WinProp™ simulation results were compared to measurements of the radiation from nine NextNav™ towers radiating at 926.227 MHz and located at various positions around the Center [14]. A simulation was performed for the area over the Center at 2.82 m AGL. A signal analyzer on a van was then driven around the Center streets with the receiving antenna mounted on its roof and the received power was recorded. A favorable comparison of simulated to measured power is shown in figure 8.

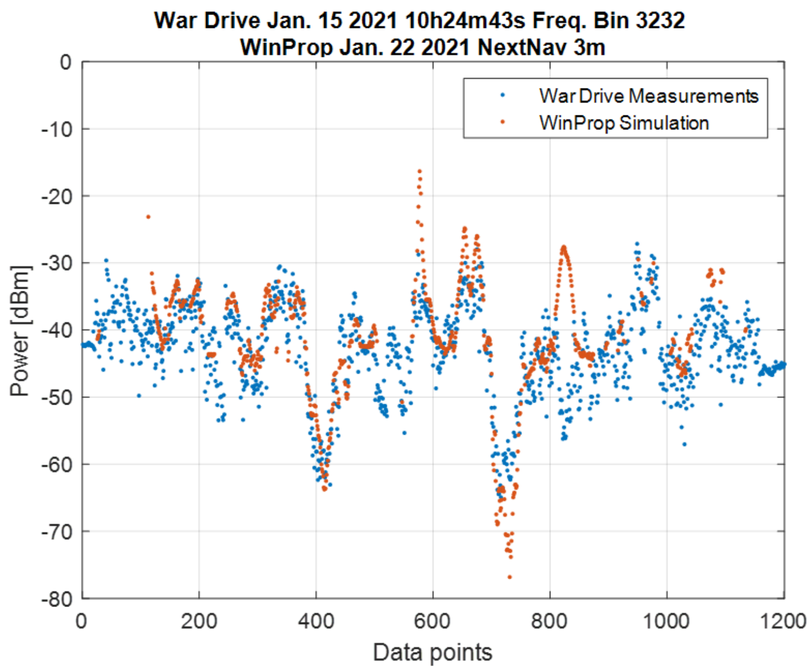


Figure 8. Comparison of simulated with measured NextNav™ 926 MHz transmitter power encountered by a van driving around the LaRC campus [14].

### *Putting REMs in Operational Context*

The initial step to putting a REM in context for drone and PAV operators is to apply a gradient to the map to create isocontours. The contours give geographic delineation to the RF power levels which serve as the basis for comparing with a flight path to identify any hazards. The contour maps then need to be stored in a way which facilitate search, update, and retrieval.

Like the REM creation, the CEM tool choice has a large influence on the process of applying a gradient to the REM. WinProp™, in this case, produces REMs in XML format which lends itself easily to creating isopower contours. The XML files include metadata to facilitate georegistration of the contours. The Python code written for this task applies up to 30 power levels on a dB scale. The number of levels in the gradient is the subject of further studies. Some optimization logic is included to speed up the processing by eliminating lower power areas or small areas. Figure 9 shows the result from applying a gradient to an REM using color coding to indicate the field level of the enclosed area.

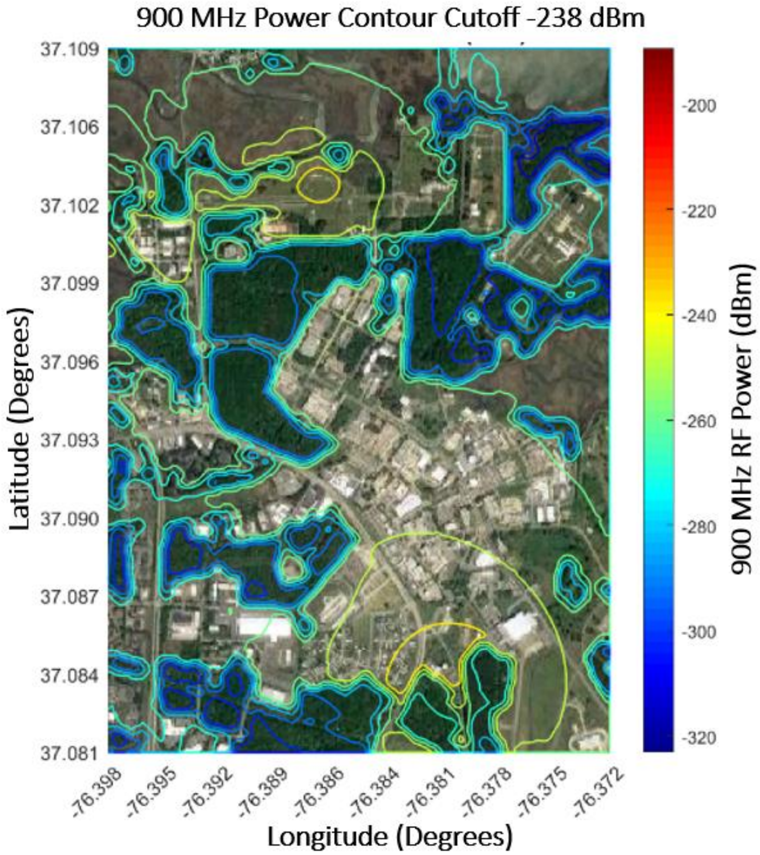


Figure 9. Sample REM contours computed from a 900 MHz REM. Map underlay from Google Maps™

Testing the contouring algorithm revealed that boundary areas needed additional treatment for the edge contours to close properly. An effective solution devised for this was to extrapolate the field levels at the edge of the REM. Kriging method was used to extrapolate up to 20 concentric rings external to the original REM. This allowed the algorithm to complete the gradient contours properly along the edge. Afterwards, the extracted contours were converted from their original Universal Transverse Mercator (UTM) coordinates to latitude and longitude and then formatted as GeoJSON [15] objects, each object representing an iso-contour at an RF power level. The GeoJSON structures contain decimated contour boundaries along with metadata for later correlation with the client's vehicle data to determine the hazard boundaries. Finally, the contours derived from the same REM are inserted as a group into a database for later recall.

A very simple database schema is used consisting of a table to store contour maps for each frequency. The table contains fields to facilitate search and recall such as the name of the operation area, the altitude of the map, and the time generated. Figure 10 illustrates the data marshalling. This data marshalling may be done offline or automated for periodic updates when live transmitter source detection is integrated in the service. In the illustrated cases, REMs for 900 MHz at different altitudes are run through the contouring step. The contours from each REM are inserted into the 900 MHz table as a row. This process is repeated with separate tables for each frequency (e.g. 2400 and 5800 MHz).

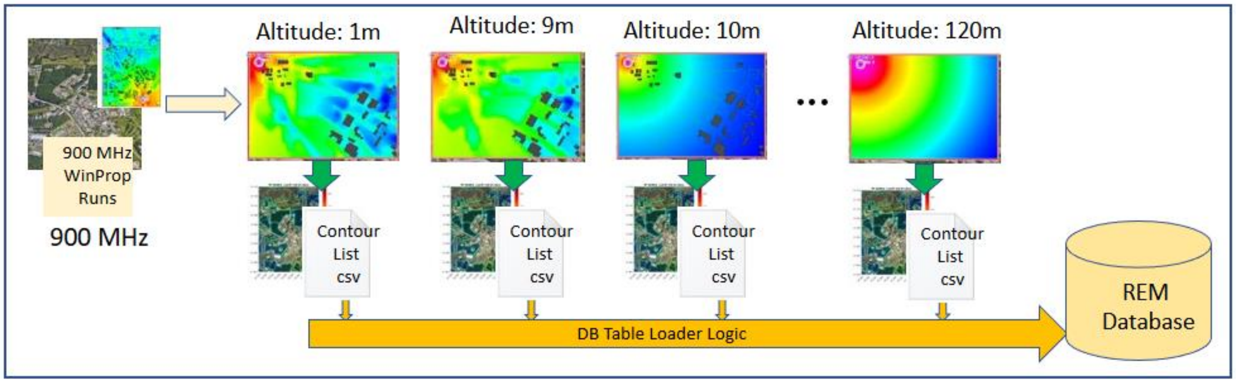


Figure 10. Data marshalling for inserting REM contours into a repository. Map underlays from Google Maps™

### *Client Interaction and Results*

The REM approach for RFI mitigation is envisioned for use during pre-flight. A prototype of this has been implemented for the CERTAIN I range. It uses standard JSON messaging formats to interact with clients. The interaction assumes the operator uses a client-side operations planning tool to plan a mission. As part of the mission, a flight plan is defined to be flown by a vehicle. The interaction with the RFI Service to fetch REMs starts with the client sending a request message to the RFI service. Figure 11 gives an example of the URL suffix for the call from the client side with notes on the input parameters.

RFI Service API Doc:

/RFI/V1/frequency926_WinProp.freqTolerance=<tolerance>.buffer=<buffer>
So for instance, a tolerance of -46 dBm and a buffer of 9 dBm would return -46 dBm to -39 dBm contours for 926 MHz from the RFI service.

Figure 11. Example RFI service call to fetch hazard contours for a given tolerance.

The service algorithm is optimized to return only the contours which enclose areas with field levels greater than or equal to the buffered level requested by the client. The returned polygons constitute hazards for the client's vehicle. Recall in earlier discussions that the REM only gives the field levels in the flight environment. The contours returned from the RFI Service are JSON format and may be used for analysis or display. Examples of RFI hazard regions are given in figures 12 and 13.

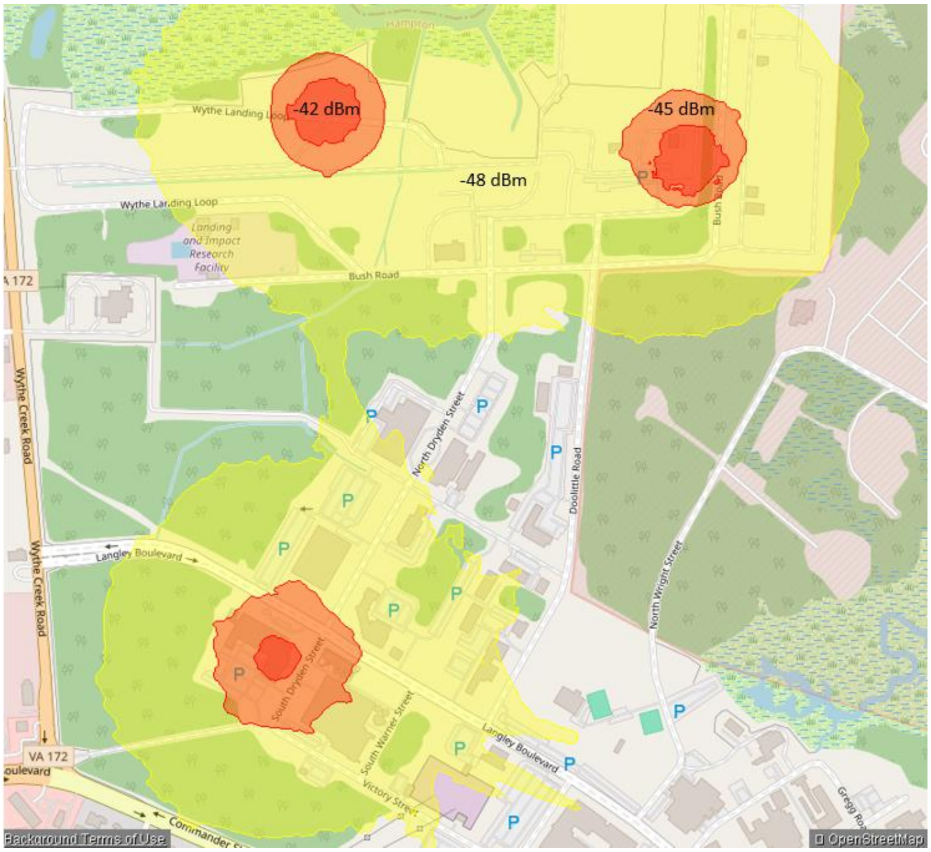


Figure 12. Example display of RFI hazard regions for a vehicle with tolerance up to -48 dBm and a buffer of 6 dBm. -48 dBm contours are shown in yellow, -46 dBm contours are shown in orange, and -42 dBm contours are shown in red. Map underlay from OpenStreetMap™

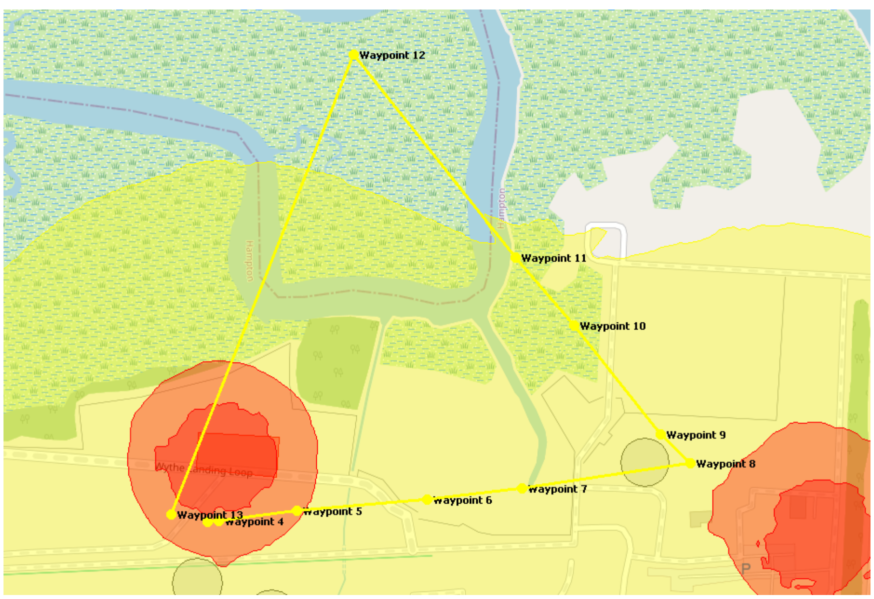


Figure 13. Overlaying the flight plan on Figure 12 gives the operator awareness of what part of the flight plan has high HIRF interference potential. Lower left of the flight plan is in red region as defined. Map underlay from OpenStreetMap™

### *Assumptions and Shortcomings*

This RFI mitigation approach is based on computing power contours from RF sources in the flying environment. Using REMs generated by a simulation tool is effective because REMs give the calculated power values for the entire flight operations space. These REMs account for terrain effects, structure blockages, multipath, or other propagation nuances in urban environments. This approach can be superior to measurement-based approaches in urban air spaces because the REMs can account for RF transmission sources embedded inside the cityscape where direct measurements are less effective due to occlusion of those embedded transmitters by surrounding buildings.

This REM approach has several detractors. The REM generation takes some compute time. Researchers prototyped a precomputed REM workflow, but a more on-demand approach might be feasible given adequate compute resources. The REM compute requires computational electromagnetic models to be developed for the flight environment. Even when building information is sourced from third parties, the material parameters need to be added. Creating and maintaining these models can be tedious, time consuming, and some assumptions must be made concerning electromagnetic characteristics for constituent construction materials used in the buildings. Creating and maintaining the models, of course, could be a revenue opportunity as well. Maintaining the source list also takes some effort.

This approach does not establish a hazard level but filters the RF power contour data to the thresholds given by the operator. Since these values are vehicle specific, it would not be practical for the server side to store threshold data for more than just a few standard vehicle configurations. From the operator's perspective, getting RF tolerance levels for the vehicle and communication link receiver sensitivity may be a challenge.

## Workflow 2: Link Continuity Hazards Mitigation Using Modeling

Communication link continuity throughout the flight path is critical to safe operation of drones and PAVs. The link enables command or supervisory control on board while providing situation awareness for operators on the ground. Loss of link continuity is often identified in the negative sense as a lost link hazard. To maintain a reliable radio communication link, it is important to have a sufficient signal-to-interference ratio (SIR). Like signal-to-noise ratio (SNR), SIR is a measure of the strength of the desired signal relative to unwanted elements in the communication system. Table 2 gives the minimum signal sensitivity for the commonly used RFD900 radio system, ranging from -94 dBm to -111 dBm, depending on the desired kilobits per second (kbps) throughput rate [16]. Note that manufacturers' sensitivity already accounts for internal noise.

Table 2. Minimum signal requirements for RFD100 radio for various throughput, from [16].

| Air data rate | Sensitivity @ 10-5 BER |
|---|---|
| 12 kbps | -111 dBm |
| 56 kbps | -107 dBm |
| 64 kbps | -105 dBm |
| 100 kbps | -102 dBm |
| 125 kbps | -104 dBm |
| 200 kbps | -98 dBm |
| 224 kbps | -94 dBm |

The RF Service calculates and displays SIR for the operator's information. SIR is the ratio of the power of the desired signal to the power of the interfering signals or unwanted signals present in the communication channel. Interference can occur due to other nearby co-frequency transmitters, reflections, multipath propagation, or other sources of electromagnetic interference. Like SNR, a higher SIR indicates a stronger desired signal compared to interference, resulting in better communication quality. The required SIR depends on factors such as the level of interference, modulation scheme, coding techniques used, and the desired data rate.

It is worth noting that the specific SIR requirements for maintaining a radio communication link vary depending on the technology, frequency band, modulation scheme, desired data rate, etc. Different communication standards have different specifications and performance requirements. Different radio brands and models may also have different SIR characteristics.

Just as in the HIRF mitigation approach, link hazard mitigation also requires vehicle specific information from the operator to determine if conditions are hazardous. Recommended SIR thresholds for the vehicle's communication may be found in the relevant technical documentation or standards for the specific radio communication system in question or can be derived from testing.

### *Link Budget Estimation Concept*

The mitigation approach taken to address link hazard is to provide operators with the prerequisite metrics for ensuring link continuity. These include the ground station power estimate over their entire flight plan and a comparative ratio of signal levels for ownship's link versus signal strength from other co-frequency transmissions. These correspond to the SNR and SIR metric previously defined. The ground station signal power lets the operator know what signal power from ownship's ground station is present along the flight path after accounting for the propagation loss through the urban environment. A comparison of this power with the communication link's minimum power requirements, such as what is given in table 2 for the RFD900, lets the operator know if any part of the flight path fails to meet the minimum power requirement.

From an RF perspective, meeting the signal power metric alone does not ensure link continuity. It is also important to know the co-frequency signal power. This is because modern communications systems almost always include an automated gain control (AGC) function to prevent a high-power signal from damaging the internal receiver and decoder circuitry. Consequently, parts of the flight path which have high SIR will likely cause the AGC to attenuate the incoming raw power and mask the intended signal. The co-frequency power and SIR information identifies those flight segments during flight planning and preflight to allow operators to adjust the flight path to reduce potential for link failure. Given adequate vehicle tracking information and workflow automation, this service may also be deployed for in-flight link health monitoring and mitigation.

In terms of protocol, this mitigation approach gives two metrics for the physical layer performance in the Open Systems Interconnect (OSI) communications model [17, 18]. Drone operators can verify physical signal continuity and signal masking. The signal power tells the operator whether the ground station broadcast has enough signal margin to reach the drone without considering other competing transmissions. The second metric compares signal margin to competing transmissions to see if masking will occur.

### *Creating the Service*

This workflow (workflow 2 per table 1) computes the RF power levels only at incremental points along the flight path. This differs from the larger workflow 1 task of computing power levels at many co-altitude points for the entire operating area. Consequently, workflow 2 is much faster and the points can be at all altitudes of the flight path. Workflow 2 entails computing two signal powers along the flight path: the power from the intended source and the aggregated power contribution from all other co-frequency sources. The SIR metric is the ratio of the two powers. The order in which these power calculations are performed is not significant and mostly dictated by the WinProp™ simulation tool employed. A list of co-frequency transmission sources is needed to calculate the SIR. Both calculations result in a set of power values along the flight path. Figure 14 shows an example plot of ground station power projected along a flight path assuming a receiving antenna having a gain of 1.5 dBi [19]. The co-frequency power can be similarly illustrated.

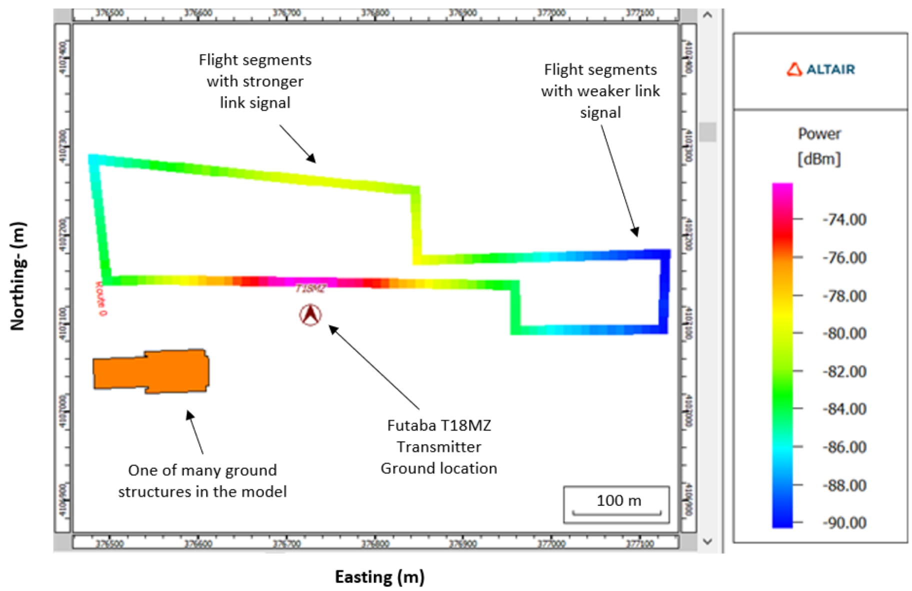


Figure 14. Simulation results for in-path power encountered by a drone from the controller on the ground while flying over LaRC. The 2.4 GHz Futaba™ T18MZ drone controller is operating at the ground station location.

### *Automating the Modeling Workflow*

Researchers also employed WinProp™ to automate this power calculation. An example of the workflow is given in [19]. For these calculations, WinProp™ is given a model of the airspace, the flight plan for the mission, and ground station transmitter information. The airspace model is the same model described for workflow 1 except that the material parameters for the objects in the model are tailored to the frequency of the vehicle's communications links. The flight plan consists of a list of waypoints the vehicle will fly. The transmitter information includes location, transmit power, and antenna patterns for the ground station.

Figure 15 illustrates the server-side automation of the workflow described in [19]. Each call to the server side calculates the ground station transmit power and the co-frequency power for one frequency. The operator's client tool makes a standard JSON call to the server with the required input information. On the server side, the operator's transmitter information is added to the list of transmitters which include other known co-frequency transmitters in the modeled space. As illustrated, WinProp™ performs the power calculations in one call but outputs the power at the flight path from each source separately. The total power for interfering signals is combined in post processing. The SIR is the ratio of the two power calculations. The interpolation distance between flight plan waypoints is set to 10 meters but can be adjusted. The results of the power calculations from WinProp™ are in text form but are illustrated in the diagram as flight paths for intuitive understanding. The data marshalling step puts the output data in JSON format for transmission back to the client. Vehicles using multiple communications frequencies would make one call to the server for each link frequency.

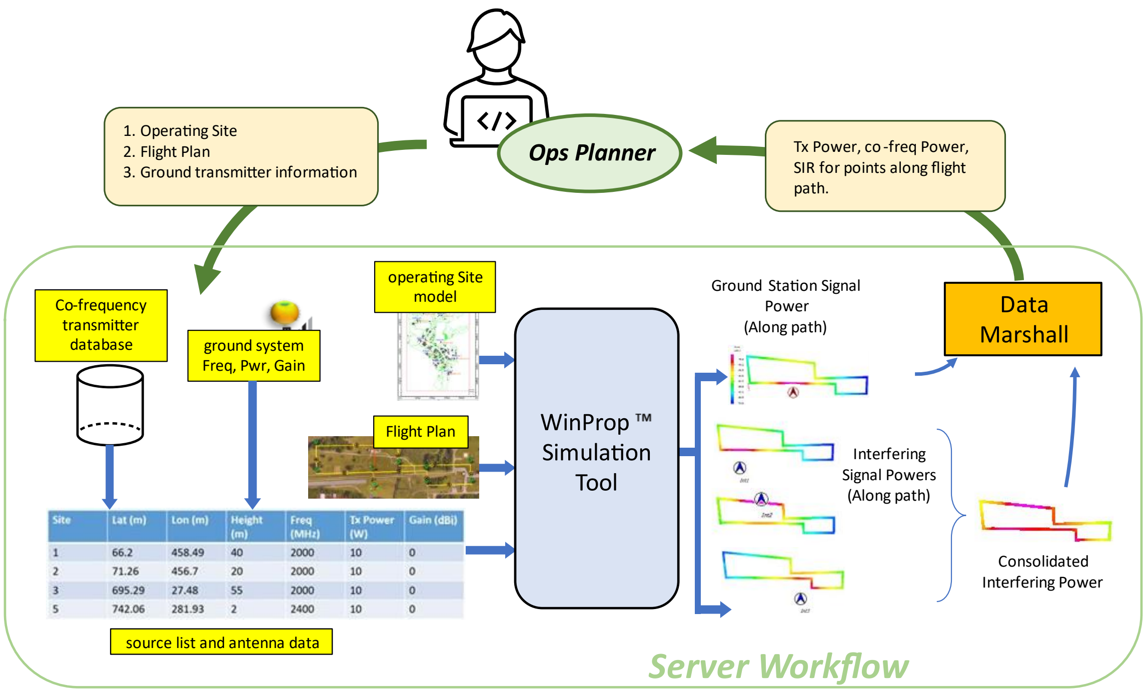


Figure 15. Server-side workflow for computing link power and SIR metric to mitigate lost link hazard. Map underlay from Google Maps™

### *Prototype Results*

A prototype of workflow 2 is implemented in the CERTAIN I Range RFI service which uses standard JSON messaging to interact with a client tool like Ops Planner or GroundWatch. A use case is illustrated next for a 900 MHz link commonly used for the ground station to communicate with on-board systems. Referring to the workflow model given in figure 15, figure 16 is an exemplar of the message objects passed from the operator tool to the service and the reply message from the server. The client request consists of range name, transmitter information, and flight plan. The service returns the power and SIR metrics for points along the flight path. The returned points include added points which are interpolated between the given flight plan waypoints. The interpolation distance is set to 10 meters. It is anticipated that the operator's tool will perform the thresholding logic to determine the minimum required power and SIR.

**Request Message from Client**


```
{
    "operating_range": "certain1",
    "comTransmitter": {
        "Latitude": 37.0983,
        "Longitude": -76.38501,
        "CoordinateFormat": "WGS",
        "Altitude": 10.0,
        "AltitudeUnits": "m",
        "ETA": 1625684522416,
        "Freq(MHz)": 926,
        "txPower": 40,
        "txPowerUnits": "dbm"
    },
    "flight_plan": [
        {
            "Latitude": 37.0983,
            "Longitude": -76.38501,
            "Altitude": 10.0,
            "ETA": 1625684522416
        },
        {
            "Latitude": 37.09851,
            "Longitude": -76.38552,
            "Altitude": 10.0,
            "ETA": 1625684532593
        },
{ . . . },
{ . . . }
    ]
}
```


**Reply Message from Service**


```
{
"freq_926_inpath_rfi": [
{
"Altitude": "10.00000",
"Interfering Power": "-48.7164",
"Interfering Signal Ratio (db)": 79.0694,
"Latitude": 37.09834120516933,
"Longitude": -76.38511006663086,
"PIC Power": "30.353000"
},
{
"Altitude": "10.00000",
"Interfering Power": "-48.7164",
"Interfering Signal Ratio (db)": 79.0694,
"Latitude": 37.09834532553714,
"Longitude": -76.38512007329547,
"PIC Power": "30.353000"
},
{
"Altitude": "10.00000",
"Interfering Power": "-48.7164",
"Interfering Signal Ratio (db)": 79.0694,
"Latitude": 37.09834944599422,
"Longitude": -76.38513007996279,
"PIC Power": "30.353000"
},
{ . . . },
{ . . . }
]
}
```


Figure 16. Example messages passed between client and server for mitigating lost link hazard.

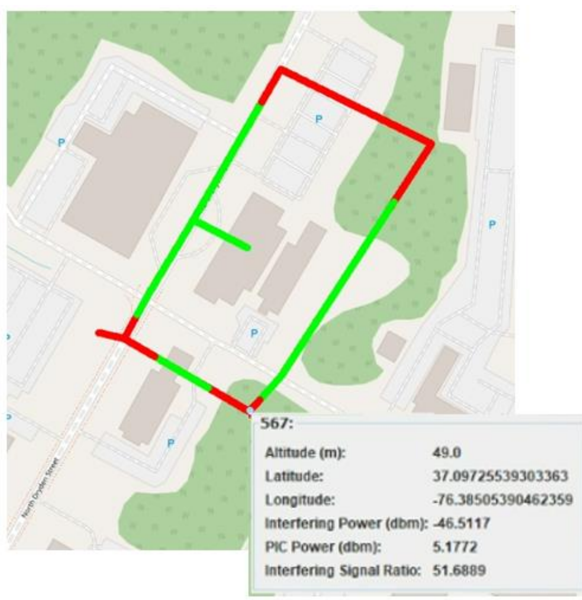


Figure 17. Lost link hazard assessment display for 926 MHz for a flight flown at CERTAIN I range where minimum signal requirement is artificially elevated to demonstrate the filter logic. Map underlay from OpenStreetMap™

Figure 17 gives the link power results for a flight flown in the CERTAIN I range. The rectangular flight path takes off from the roof of a building, encircles two buildings, and crosses over an adjacent building. The path traverses near and over several wooded areas and has a landing segment in a grassy area. The computed received power is in the range of 5-7 dBm which is more than adequate for the 900 MHz link used. For illustration purposes, the minimum receiver power was set to 6 dBm to illustrate the filtering logic for marking the part of the flight path which would have difficulty maintaining link continuity. The link hazard threshold in this case is set to locations where the link power is less than the threshold (6 dBm in this illustration) and SIR is greater than 10 dB. This GroundWatch operator tool overlays the flight path on an Open Street Map™ (OSM) for landmark registration and allows the operator to float over each point and get numerical values for the link hazard metric.

### *Applicability to Urban Environment*

Link loss is of great concern for urban UAS and PAV operations because of the complexity of the urban RF environment. Using a model-based approach to address link lost hazard is ideal because the models may be created for any flying area without requiring installation of an RF monitoring system. The models can account for signal loss through urban structures. The CEM simulation software can also account for the proliferation of transmitters, present in the urban environment, that may be using the same frequency as the vehicle's link with its ground station. The simulation gives the physical signal power along the flight path, which the operator can intuitively translate to link continuity or, inversely, link lost. Providing the information during flight planning allows operators to adjust the flight path before executing the mission.

### *Assumptions and Shortcomings*

Workflow 2 has detractors similar to workflow 1. It requires models for the urban operations space. Creating and updating the buildings and features in these models is somewhat resource intensive. Also, there needs to be multiple models to cover frequency ranges for which electromagnetic characteristics are different enough to significantly impact the calculated results. But only one model of each frequency band needs to be created, as both workflow 1 and workflow 2 can use the same model for a given frequency band of interest. On a positive note, this is also a revenue opportunity for a company to produce and maintain these models in much the same way that Jeppesen sells subscriptions for approach plates to airports worldwide.

Another difficulty in fielding this approach is maintaining the list of transmitters in the flight environment. This is needed to create the list of co-frequency transmitters for the SIR metric. To some extent, this is made easier by the FCC publication of licensed transmitters. That information can be assimilated with measurements in the operation area, if available, to compile a more accurate list of transmitters in the operating space.

## Workflow 3: Mitigating Link Loss Using Live Spectrum Monitoring

Where spectrum monitoring capabilities are available in the operating area, another measurement-based approach can be employed to mitigate link loss hazard. One such approach gives a spectrum occupancy (SO) metric to determine air waves congestion. The SO metric provides necessary information additional to the signal power from workflow 2 to assess link hazard for a UAS mission. It is useful for scenarios in which multiple UAS in the same area are using the same communications systems, allowing multiple parties to communicate at the same time. Specifically, SO assesses congestion in point-to-point connections that use frequency and time domain multiple access (FTDMA) protocols, now common with even low-cost RF communications systems. Only a summary description of the SO metric is given here. More information on measurement and computations of spectrum occupancy may be found in [20, 21]. The following section describes application of the metric to link hazard mitigation.

### *Spectrum Occupancy Estimation Concept*

Modern communications systems allow multiple operators flying in the same area to communicate with their respective drones using links that operate over the same frequency band. With FTDMA, transmissions from the operators are multiplexed in time and specific channel frequencies defined within that band. Consequently, there is a limit to the number of transmissions which can be made during each transmission period without crosstalk. In simple terms, the number of available transmission slots is the number of channels defined in the transmission hardware times the epoch size where the epoch size is a number of transmission periods. The SO metric gives the ratio of the number of transmission slots used over the number of transmission slots available for the selected epoch. Ignoring intricacies of hardware error correction and robust protocol, the SO characterizes how busy the airwaves are during an observation epoch. Depending on hardware and protocol configuration, high SO may manifest as slow link response between communication end points or frequent broken links. Operators can mitigate this link hazard by establishing an acceptable SO percentage under which flight may be conducted. The exact "No fly" decision threshold depends on the hardware and the operator's risk posture.

The message traffic between the vehicles is arbitrated in the protocol layers. Figure 18 shows the theoretical, 7-layer, OSI representation of modern communications between drones and ground stations. From the OSI perspective, the spectrum occupancy (SO) assesses the shared bandwidth used by multiple UAS operations. SO gives some notion of the amount of congestion of the shared link resource at the datalink layer. This differs from workflow 2, which assesses the reach and masking at the physical layer. Figure 18 shows the RFI mitigation approaches relative to the OSI model.

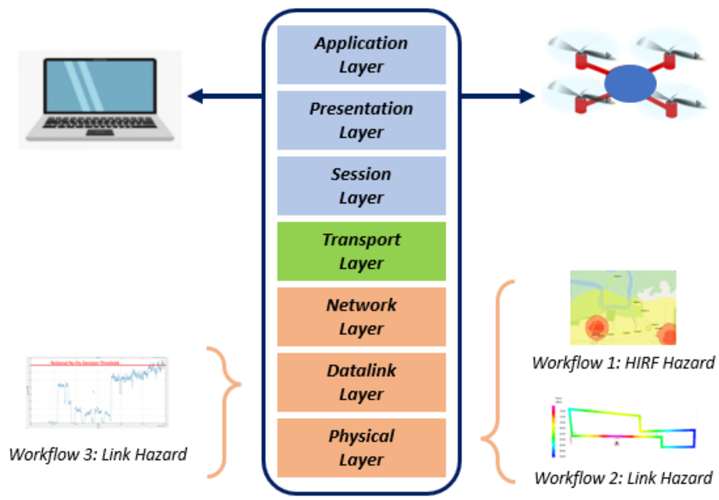


Figure 18. Layers in the ISO's theoretical OSI model [22]. Map underlay from OpenStreetMap™

For mesh and FTDMA-based communications systems, even if the workflow 2 metrics (adequate signal power, no co-frequency masking) are satisfactory, a link continuity hazard may still exist if the bandwidth is heavily shared by others operating in the area. This hazard manifests as slowly arriving or lost message frames due to heavy use of the bandwidth. Message frame delivery can slow to the point where the message assembly layers time out waiting for all the frames to assemble a message. This causes the protocol layers to report broken link diagnostics to their upper application layers.

### *Spectrum Monitoring*

SO can be derived from direct monitoring of the spectrum environment in the operating area. Researchers integrated the RF monitoring system at the CERTAIN I range into a 5-node network. Figure 19 shows the locations of RF sensors (red dots) throughout the CERTAIN I range. Testing for this workflow was primarily in an area circumscribed by the Mobile, Pyro, and Old ALDF Shop nodes. These nodes were configured to monitor the spectrum in the frequency of interest.

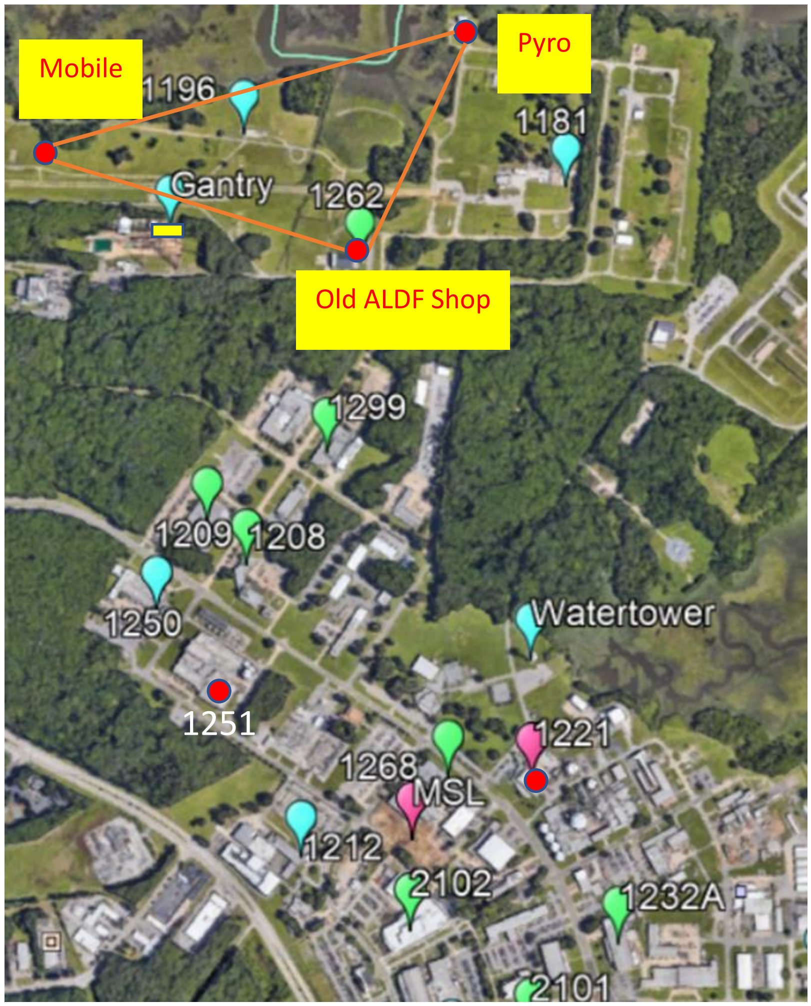


Figure 19. The yellow tags identify three of the five CRFS nodes used in RF bandwidth monitoring in the CERTAIN I Range. Map underlay from Google Maps™

The CRFS's RFeye Mission Manager™ software facilitates querying live or logged spectrum data. Figure 20 shows a waterfall plot for a spectrum recording during which spectrum occupancy testing was performed on the RFD900 communications link. The CRFS nodes were set to monitor 900-930 MHz. The primary test link was an RFD900 system configured to use only 902 to 915 MHz. A second communications link channel was tested at 915 to 930 MHz. The 920-930 MHZ spectrum was actively used by another system during this test. It is easy to see that there is interference in the 920-930 MHz region from the conflict with another user of that band. Consequently, the second link fared poorly with multiple broken links.

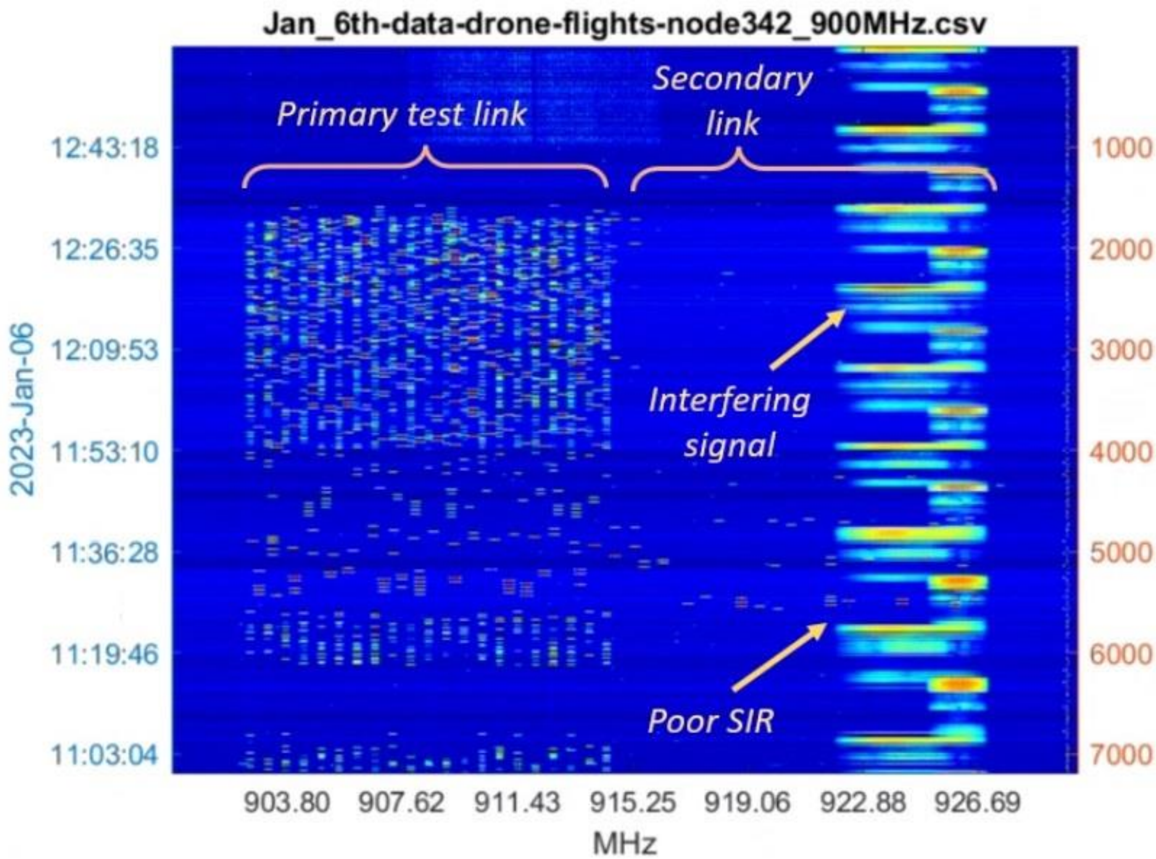


Figure 20. Waterfall recording of message transmissions in the 900 MHz band at the CERTAIN I Range during test measurements.

### *Spectrum Occupancy Computation*

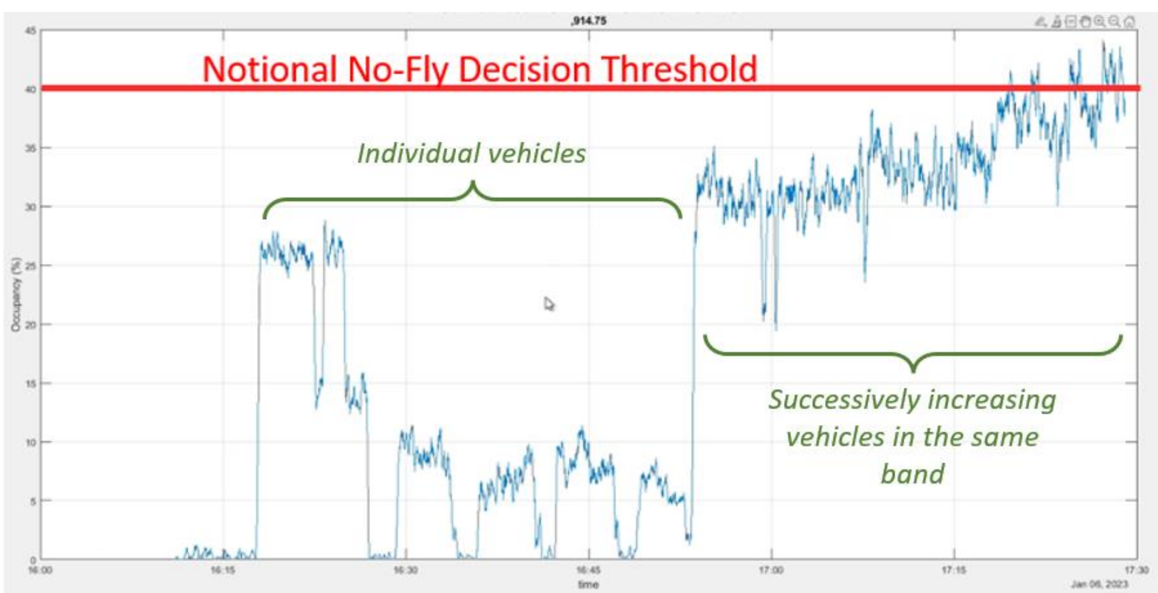


Figure 21. Spectrum occupancy from individual and multiple users of the same frequency band.

The SO metric is expressed as a percent, calculated from monitoring the spectrum over a defined time window from continuous measurements. The algorithm used is a variation of the one used by the International Telecommunication Union (ITU) in urban spectrum monitoring tests. Results of the SO calculations are summarized here; [21] gives more details on the test and formulation. Figure 21 shows the spectrum occupancy from the test data in figure 20. The test used five UAS communicating on the same 900 MHz band with similarly configured RFD 900s. As seen in the plot, the first segment of the test includes only individual vehicles communicating. The first vehicle is set to a higher message rate. The second segment of the test shows the increase in spectrum occupancy as successively more vehicles are operating at the same time. This workflow, like previous workflows, does not prescribe a bandwidth threshold for link hazard. The proper threshold to use is dependent on the protocol and may even depend on the configuration of the RF link hardware. As in prior mitigation approaches, the threshold must be provided by the operator.

### *Creating the Service*

Researchers have implemented the spectrum occupancy metric for the RFD900 system. The request and reply message is given in figure 22. Note that there are provisions in the message design to accommodate other frequencies and protocols. An exemplar display of the SO metric is given in figure 23, where the calculated occupancy data are displayed on a map. Using a thresholding value to determine a good or bad occupancy percentage, the nodes can be color coordinated to indicate bad or good occupancy values. This is a measurement-based metric and so the usefulness of the metric is attached to the geographic points of measurement, which are the receivers in the RF monitoring system. The uncertainty of the metric is increased radially from the point of measurement. There is no technical basis for extrapolating the metric beyond the point of measurement. It was observed during the testing that the sensing nodes farther away from the transmitting source had a lower SO metric during the testing.

**Reply Message from Service**


```
{
"AirOccupencyPercent" : {
"agc" : "TRACKING",
"loops" : 16,
"nodes" : [ {
"Pyro" :[ {
"2400" : [ { "OCC_Percent" : "N/A" } ],
"5000" : [ { "OCC_Percent" : "N/A" } ],
"900" : [ { "OCC_Percent" : "1.57%" } ],
"GPS" : { "altitude" : 13.086, "latitude" : 37.105913, "longitude" : -76.383017 }
} ],
"mobile" : [ {
"2400" : [ { "OCC_Percent" : "N/A" } ],
"5000" : [ { "OCC_Percent" : "N/A" } ],
"900" : [ { "OCC_Percent" : "7.65%" } ],
"GPS" : { "altitude" : 11.055, "latitude" : 37.102629, "longitude" : -76.393158 }
} ],
"old_LDEF_shop" : [ {
"2400" : [ { "OCC_Percent" : "N/A" } ],
"5000" : [ { "OCC_Percent" : "N/A" } ],
"900" : [ { "OCC_Percent" : "3.53%" } ],
"GPS" : { "altitude" : 7.91, "latitude" : 37.101663, "longitude" : -76.384866 }
} ]
} ],
"range" : "certain1",
"resolution_bandwidth" : 15293.0,
"timestamp" : 1.681332678245105E9,
"unit" : "POWER",
"vehicleName" : "aragog"
}
}
```


Figure 22. Request and reply message for SO information from the RFI service.

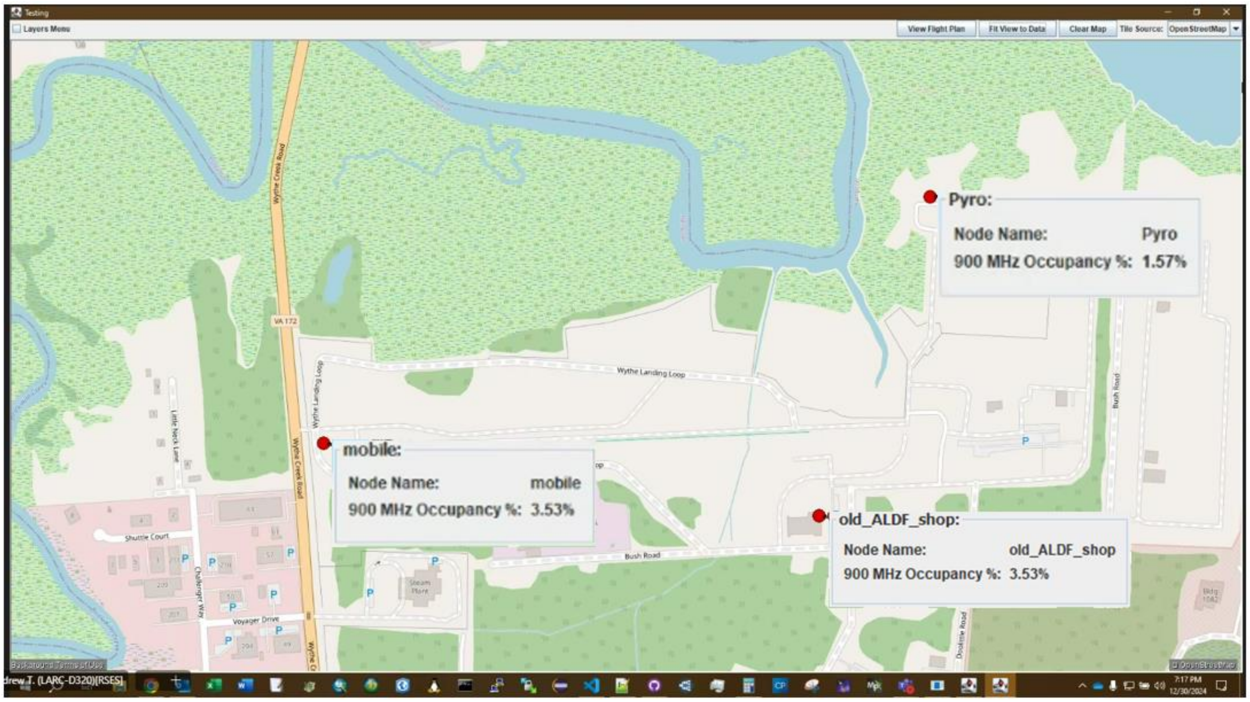


Figure 23. Operator's display of SO information from the RFI service. This was not during the test measurement. Map underlay from OpenStreetMap™

### ***Strengths and Weaknesses of this Approach***

One of the shortcomings of measurement-based approaches is that the metric is valid and real only at the locations where the monitoring system has antennas to probe the RF environment. Unless the operating flight plan is in the close vicinity of the measurement point, the operator is left to extrapolate from that measurement point out to the flight path and determine how much the metric will impact the vehicle along the flight path. This extrapolation is not likely linear and any assumptions about applicability of the metric can be very problematic in complex urban environments.

This is a protocol-specific approach. The algorithm for bandwidth will vary a bit based on the protocol. One of the difficulties of using this mitigation approach is that owners of proprietary protocols are sometimes hesitant to release the technical data to allow an independent derivation for their bandwidth sharing schemes.

Measurability is another weakness in this approach. During testing, it was found that some of the CRFS nodes did not receive enough signals to discern the spectrum usage. This was potentially due to the height of the receive antenna installations and occlusion of the vehicle transmissions by nearby trees and buildings. These conditions are like conditions that would be encountered in urban installations where placement of RF monitoring antennas is difficult and blind spots behind tall structures are common.

### **Workflow 4: Mitigating In-Band Interference using Spectrum Monitoring**

Spectrum monitoring in the operating environment can provide historical trends as well as current measurements for environment metrics. Another mitigation approached explored is to use historical spectral power data collected at frequencies of interest to identify times of elevated RF radiation which may correlate to higher probability of HIRF and communications link hazards. This approach is like workflow 1 where a model is used to geolocate the RF power level in the flying environment. The raw metric for this mitigation approach is the periodic measurements of the RF spectrum with regression analysis to allow projections into the future. As with all other approaches, the threshold at which the measured power indicates a no-fly condition depends on the sensitivity of the UAS and the risk tolerance of the operator. The advantage of this approach over workflow 1 is that this is based on measurements from each sensor, which reflect existing conditions as opposed to a model of the environment.

### *Raw Spectrum Power*

The RF monitoring system installed in CERTAIN I is configured to log synchronous sweep scans to sample maximum RF power across the frequency bands of interest, sampling every 15 minutes. This data can be aggregated in various ways, such as the maximum power values in specified time spans (hourly, daily, …), to make the information more manageable. Each power maximum represents the worst-case RFI scenario seen in the environment during the sampling period. The data can be used to feed trend analysis to extrapolate to future times; the raw RF sensor scans also give the immediate RF environment conditions.

Visualizations showing temporal relations of RF power to planned mission times give UAS operators a reference to adjust mission start times to minimize the RFI risk. Example calendar plots showing the hourly maximum power over a week and a month are given in the top two plots of figure 24. The bottom plot shows the daily maximum power over a specified number of weeks. These plots give the maximum (red blocks) and minimum (black blocks) power levels detected at one of the 5 sensor locations. This type of trending information can help operators during mission planning phase to shift the mission time or day to minimize the RFI hazard. This information can potentially be used as a preflight check or in-flight monitoring since the sensor data can reflect current conditions.

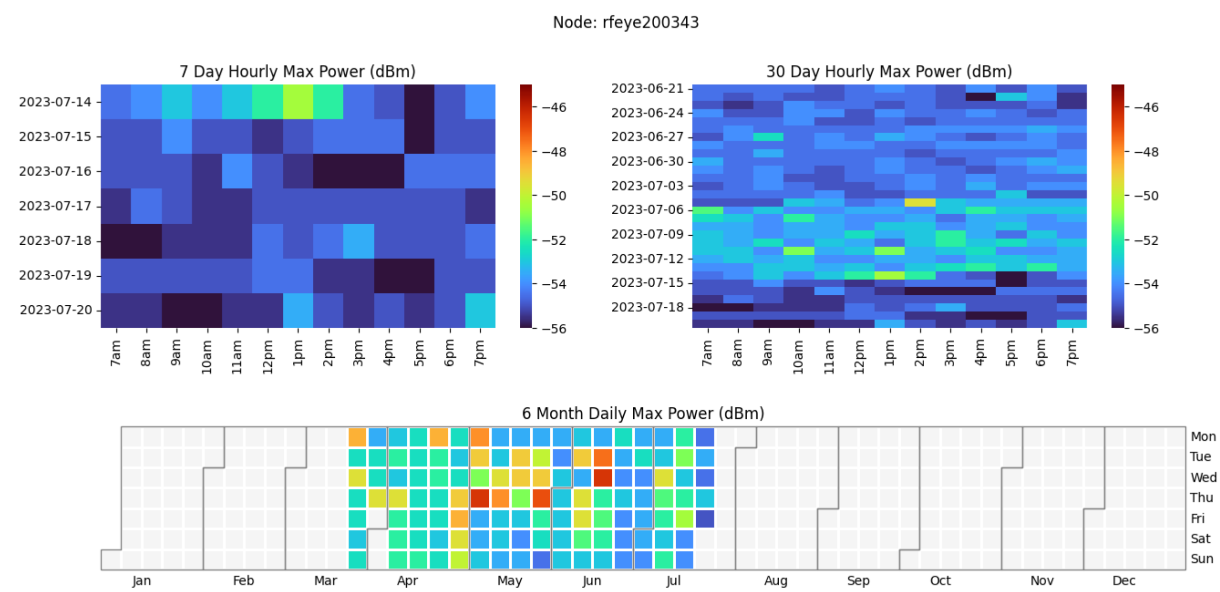


Figure 24. Examples of presenting RF power data to show temporal relations to mission operations. Maximum power data from a CRFS node over 7 days hourly (left) and 30 days hourly (right) and 6 months daily (bottom).

### *Creating the Service*

The spectrum monitoring portion of the RFI Service relies on accessing sensor measurements from the CRFS™ system, which obtains logged data samples. From CRFS nodes internal to the CERTAIN range, real-time scans are reported to a data repeater for distribution; currently the data include scans in the 900 and 2400 MHz bands. Measurements from each of the five nodes are published for both bands. Figure 25 shows examples of the data object that a subscriber may get for each node. Refinement of the regression analysis and trending algorithms for the RF spectrum reporting is still ongoing.

**Topic Name: RFEnvironmentScan/900MHz/Node1**


```
{
"api_type": "emp",
"frequency": "900",
"node_ID": "node1",
"node_name": "rfeye200342",
"building": "Trailer",
"nickname": "Mobile",
"GPS": {
"latitude": 37.10263,
"longitude": -76.393149,
"altitude": 7.784
},
"start_frequency": 899997711.182,
"end_frequency": 930004119.873,
"unit": "POWER",
"loops": 16,
"agc": "TRACKING",
"resolution_bandwidth": 15293,
"max_value": -101,
"min_value": -115.5,
"values": []
}
```


**Topic Name: RFEnvironmentScan/2400MHz/Node4**


```
{
"api_type": "emp",
"frequency": "2400",
"node_ID": "node4",
"node_name": "rfeye200340",
"building": "1221",
"nickname": "1221",
"GPS": {
"latitude": 37.093178,
"longitude": -76.380631,
"altitude": 23.312
},
"start_frequency": 2399978637.696,
"end_frequency": 2500045776.367,
"unit": "POWER",
"loops": 16,
"agc": "TRACKING",
"resolution_bandwidth": 61170,
"max_value": -84,
"min_value": -110.5,
"values": []
}
```


Figure 25. Spectrum scan data published to data repeater.

### *Strengths and Weaknesses of this Approach*

One of the strengths of this approach is that it reflects actual conditions in the flying environment because the metric is based on measured data. The measured RF power can be used for both a preflight check and in-flight monitoring. The trending and regression can be used to estimate future levels, although it should be cautioned that the correlation from the regression analysis should be taken only as a likelihood of the presence of RF in the future. The specific independent variables in the regression analysis should consider local spectrum usage.

As with other measurement-based approaches, this approach also suffers from measurability and usage factors. That is, the measurements in urban environment may suffer from occlusion. Also, the uncertainty of the measurement grows with the radius away from the point of measurement. Only a summary impact may be concluded from this data because it has to be extrapolated from the measurement point to the flight path.

## Workflow 5: Mitigating Out-of-Band Interference by Using Data Mining to Create a High-Intensity Radiated Field (HIRF) Map - An Avoidance Approach

Workflow 5 implements a HIRF avoidance approach first described by Nguyen in [23]. It combines published transmitter registration information with maximum RF tolerance for the vehicle to create a mitigation product for UAS and PAV operators. Like workflow 1, this also depends on testing or manufacturer-provided vehicle RF exposure limits.

### *HIRF Map Approach*

Vehicles operating in an urban environment face higher probabilities of encountering HIRF due to a higher concentration of transmitting sources to meet the demands of a dense population center. These HIRF transmitters include broadcast transmitters, various wireless communication technologies, and even radars from nearby airports. Even though these tend to be fixed in locations close to the ground, urban centers with seaports may also have mobile sources such as radars and communication transmitters on ships and aircraft.

Typical aircraft and helicopters are required to tolerate field levels specified in HIRF standards and regulations [5, 6, 7, 8]. HIRF environments in these test standards are mostly dominated by transmitters located near large airports, where aircraft are closest to the ground and are at risk of being illuminated at close distance. The HIRF environment for rotorcraft is more severe (higher field levels) than for fixed-wing aircraft because rotorcraft operate and hover closer to the ground in normal operation and can be directly illuminated by ground transmitters at close distances inside and outside airport boundaries.

PAVs and UAVs operate in similar HIRF environments as rotorcraft, as they fly close to the ground and can be illuminated directly by ground transmitters. As a result, these vehicles may be required to meet the same HIRF requirements. Protection against the severe rotorcraft HIRF environment could result in undesirable increased vehicle cost, size, and weight. Low-cost constructions with less shielding and filtering may make the standard certification approach difficult.

Nguyen [23] explores an alternate approach to the standard HIRF protection practice which potentially lowers the costs of HIRF protection on UAS vehicles. Rather than designing the vehicles to tolerate the HIRF environments associated with aircraft and rotorcraft standards, the proposed approach restricts vehicles from being exposed to more severe environments than they can safely tolerate. By staying away from HIRF transmitters at safe distances, HIRF tolerance could be achieved with much less protection than normally required, leading to lower design and manufacturing costs.

This RFI mitigation is based on providing the operator with a HIRF avoidance map tailored for a given vehicle's HIRF tolerance level. Flight maps geolocate transmitters in the vicinity of the flight operation and provide "stay-out" regions around the transmitter locations. The safe standoff distances and avoidance zones are computed and plotted onto maps to set operational boundaries so that the vehicle's field tolerance level is not exceeded. Higher transmit power from an antenna results in a larger HIRF zone. This concept is generalized and termed as a HIRF Map. Figure 26 gives a notional illustration of using the HIRF Map concept. Given the information during flight planning, the pilot may route the vehicle around known HIRF sources, ensuring the flight path is well outside of the tailored HIRF zones to observe the vehicle's HIRF tolerance.

A vehicle's tolerance levels can be determined from testing and analysis. HIRF transmitters' data may be obtained from national spectrum regulatory agencies, including the Federal Communication Commission (FCC) and the National Telecommunications and Information Administration (NTIA) in the United States. Databases from the FCC are publicly available, while databases from the NTIA contain government spectrum use and are proprietary.

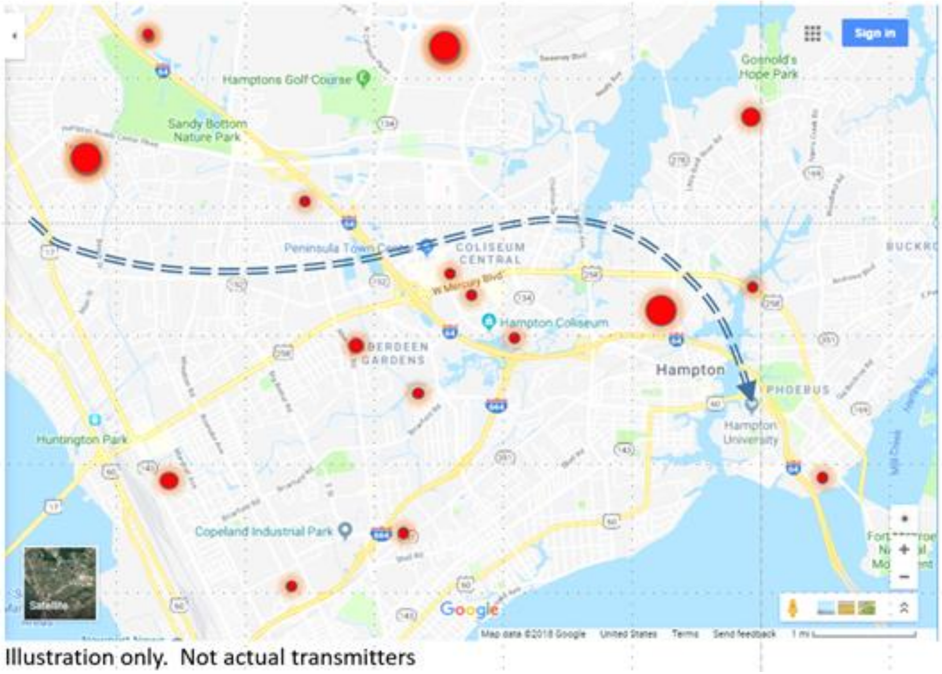


Figure 26. Planning flights around HIRF transmitters.

For common transmitters such as microwave links, pagers, land mobile radios, and cellular/wireless towers, it is recommended that the vehicle can tolerate a certain field level corresponding to a safe distance. This recommendation minimizes the complexity of dealing with the numerous transmitters in an urban area. The tolerance level is suggested to be about 20-25 V/m below 2 GHz (or even lower in some bands), and 50 V/m above 2 GHz at the minimum distance of 100 feet [24]. This 100-foot distance was used in the HIRF environment calculations [5]. It is also recommended that the vehicle can tolerate portable transmitters operating in its vicinity.

### *Creating the Service*

The transmitter HIRF Map service is first initialized by instantiating a live schema of the FCC database for transmitters. The FCC data gives location, types, and emitted power for transmitters in various categories. Each category is stored in a separate table. The data is downloadable from FCC repositories on a daily or weekly basis. [23] describes this process in detail and gives a Matlab™ implementation to import the FCC transmitter databases and other transmitter sources. Figure 27 illustrates the process. The green boxes are data input; blue boxes are calculations. The gold box represents the interface with flight planning software. Once the schema is live (left green box), the client can get the HIRF map as follows:

1) Client sends service request with operation location (top green box), and vehicle HIRF tolerance information (right green box).
2) Server can search for transmitters in the vicinity of the operating area which transmit in the given HIRF bands.
3) Server computes the stay-out radius around the transmitters meeting the criteria.
4) Server replies with transmitter and stay out radius information to the client.
5) Client displays geo-located stay-out regions for operator to determine if flight path needs adjustments.

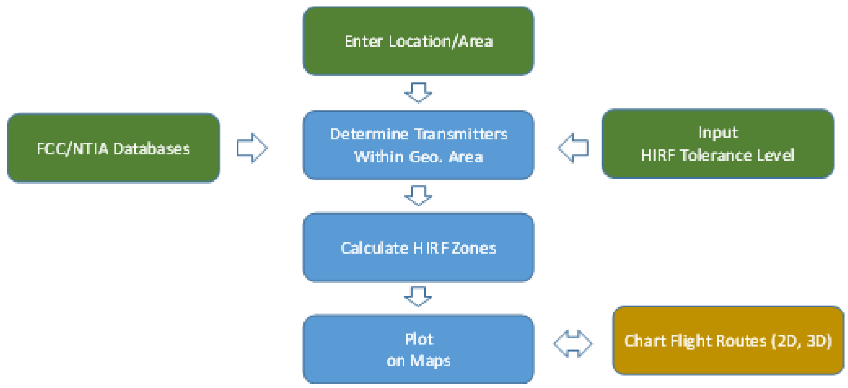


Figure 27. HIRF Map process.

The server calculation makes worst-case assumptions about antenna direction, gain, and power from the FCC data to arrive at a conservative estimate for the stay-out radius. The regions outside of the stay-out radius in theory represent the regions of lower interference risk from the transmitters.

### *Results*

An example of the result is illustrated in figure 28 showing HIRF zones of satellite ground transmitters for a vehicle having a 10 V/m tolerance level. The fan-shaped zones represent the possible scanning angle by the transmitter. HIRF zones for transmitters without scan angle data are shown as circles to be conservative.

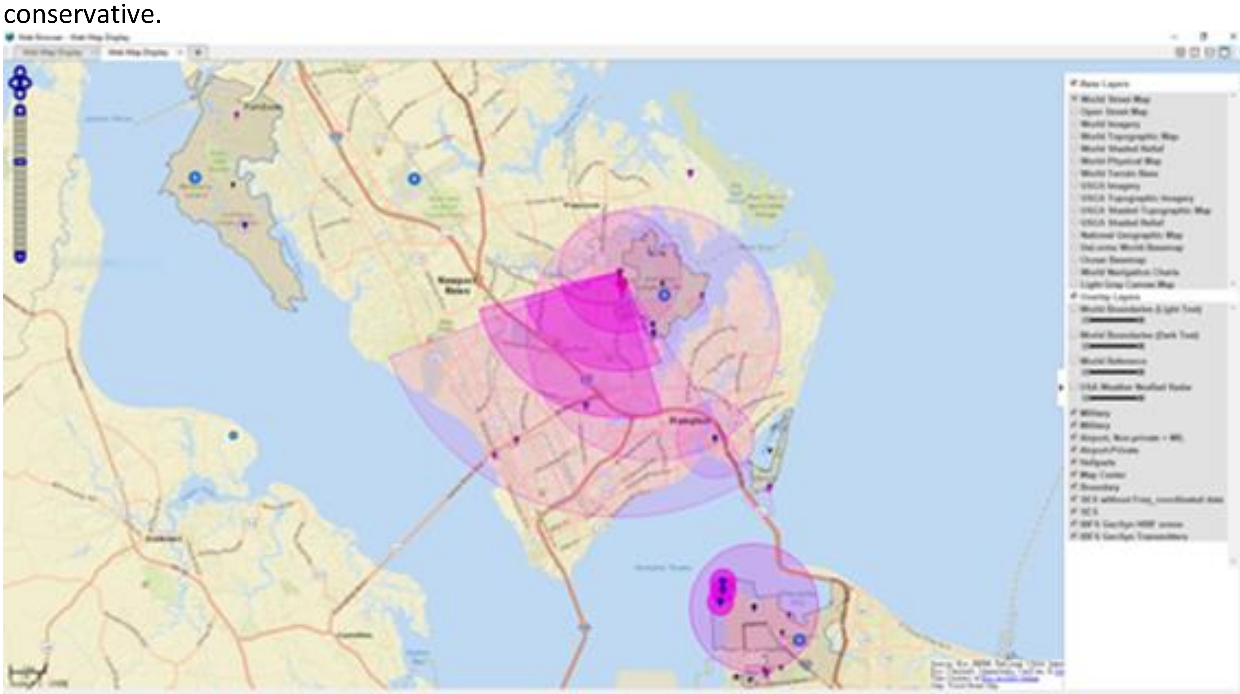

Figure 28. Example of HIRF zones of satellite ground transmitters. Map underlay from Matlab Web Map™

### *Strengths and Weaknesses of HIRF Map Approach*

This approach is attractive because the transmitter data is readily available for download. The data is a bit arcane, but the database schema updating can be automated. It should be noted that the data does not include cell tower locations because the FCC does not require cell tower owners to report the location of their towers. Additionally, the cell tower information is competitor sensitive and not easily available. Hence a minimum tolerance requirement is recommended in the previous discussion.

Another advantage in this approach is that it may be used during flight to manage RFI safety when the vehicle trajectory must deviate from the original flight plan due to other factors. In that case, the vehicle's automated decision control logic can transact directly with the RFI service or send the trajectory change to the ground station for checking to see if mitigation action is needed or if the trajectory change will introduce RFI risks.

This approach for RFI mitigation suffers from the same detractor as the workflow 1 REM approach. That is, it requires some notion of the HIRF levels and frequencies to which the vehicle is sensitive, either from manufacturer information or from a community-set standard. In the latter case, the manufacturer of the drone or communications equipage will also need to verify that their equipage can survive the community-set threshold requirements. Lastly, a one-size-fits-all threshold may not be economically viable for smaller drones with severe size, weight, and power constraints.

## Conclusion and Future Work

In this work, researchers have identified HIRF and link loss as primary types of RF interference hazards that can jeopardize drone or PAV flight operations. A brief treatment is given of the critical factors and modes of entry which combine to create hazardous interference conditions. Closer examination of these reveals that knowledge of RF frequency and power encountered by the vehicle is essential to deploying ground-based RFI mitigation solutions. Throughout this work, it is discovered that the exact value of frequency and power for establishing a hazardous threshold depends on vehicle communications equipage and the sensitivity of the on-board electronic configuration to random coupling of RF energy. This necessitates that RF Service users provide vehicle-specific frequencies and power thresholds along with planned vehicle trajectories in order for the RFI mitigation solutions to be meaningful for specific vehicles or operations being executed.

Five approaches are devised to mitigate HIRF and link loss hazards in urban flight operations. Early research focused these approaches on providing link or environment information in the context of the vehicle or operation so that hazards are discovered, and mitigations taken during flight planning or pre-flight phases. Potential for in-flight use of some of the approaches is examined where applicable. Both model and measurement-based approaches are explored with some consideration to their strengths and weaknesses. Link hazards may be alleviated in part by providing operators with model-calculated link power along the flight track (Workflow 2) and current or historical bandwidth occupancy measurements from the operations area (Workflow 3). HIRF hazards may be addressed by providing operators with delineated RF stay-out areas calculated either from urban environment maps (Workflow 1) or calculated from transmitter registration information provided by the FCC (Workflow 5). Alternatively, operators could make a risk assessment based on regression analysis of historical spectrum measurements (workflow 4).

Much work remains in several areas to perfect these ground-based RFI mitigation solutions. Determining the accuracy and effectiveness of these approaches will require further in-flight and down-range measurements to compare with models. The usable range of the measured safety metric should be examined. Practical improvements are still needed for making accurate urban models and identifying electromagnetic characteristics of construction materials in the urban model. While significant work has been done in the prototyping, additional user testing would help identify workflow optimizations – especially in workflow 5 which depend on periodic updates from external information links.  Lastly, little work has been done to examine the user presentation of the RFI mitigation information.

# References


1. Young, Steven D.; Ancel, Ersin; Moore, Andrew J.; Dill, Evan T.; Quach, Cuong C.; Foster, John V.; Darafsheh, Kaveh; Smalling, Kyle M.; Vazquez, Sixto L.; Evans, Emery T.; Okolo, Wendy A.; Corbetta, Matteo; Ossenfort, John P.; Watkins, Jason; Kulkarni, Chetan S.; and Spirkovska, Lilly, "Architecture and Information Requirements to Assess and Predict Flight Safety Risks During Highly Autonomous Urban Flight Operations," NASA/TM-2020-220440, January 2020. https://ntrs.nasa.gov/api/citations/20200001140/downloads/20200001140.pdf
2. Ellis, Kyle; Krois, Paul; Davies, Misty; and Koelling, John, "In-Time System-Wide Safety Assurance (ISSA) Concept of Operations," Document ID 20190032480, Report Number ARC-E-DAA-TN4516-1, October 31, 2019.
3. Li, Jilu; Gomez-Garcia, Daniel; Rodriguez-Morales, Fernando; and Leuschen, Carl, "Evaluation of Front-Door and Back-Door RFI Impacts on Small UAS Operation Safety," IEEE International Symposium on Electromagnetic Compatibility (EMC), Grand Rapids, MI, July 29, 2023.
4. Li, Jilu; Gomez-Garcia, Daniel; Rodriguez-Morales, Fernando; and Leuschen, Carl, "Testing and Assessment of Small Unmanned Aerial Vehicle Susceptibility to Environmental Radio Frequency Interference," *IEEE Transactions on Electromagnetic Compatibility*, vol. 66, no.3, pp. 728-748, 2024.
5. SAE Aerospace, Aerospace Recommended Practice (ARP) 5583A (EUROCAE Document ED-107A), "Guide to Certification of Aircraft in a High-Intensity Radiated Field (HIRF) Environment," June 2010.
6. RTCA/DO-160D, "Environmental Conditions and Test Procedures for Airborne Equipment," July 29, 1997.
7. FAA Rule, "High-Intensity Radiated Fields (HIRF) Protection for Aircraft Electrical and Electronic Systems," 72 FR 44015, Docket No. FAA-2006-23657, August 06, 2007.
8. FAA Advisory Circular (AC) 20-158A, "The Certification of Aircraft Electrical and Electronic Systems for Operation in the High-Intensity Radiated Fields (HIRF) Environment," May 30, 2014.
9. FCC Rule, "Spectrum Rules and Policies for the Operation of Unmanned Aircraft Systems," 90 FR 1830, WT Docket No. 22-323, Report and Order, August 21, 2024.
10. "CRFS Spectrum Monitoring and Geolocation," https://www.crfs.com/
11. The University of North Dakota, The University of Kansas, and Drexel University, "Evaluate Unmanned Aircraft Systems (UAS) Electromagnetic Compatibility (EMC)," ASSURE Report No. A56-A11L.UAS.96, June 9, 2023. https://www.assureuas.org
12. Makarchuk, Roman, "Drones in Telecom Operations: A Guide to Drones and Telecom," *Intellias*, October 04, 2024. https://intellias.com/drones-in-telecom/
13. "How to Inspect a Tower Using a Drone?" *Hammer Missions*, November 4, 2022. https://www.hammermissions.com/post/how-to-inspect-a-tower-using-a-drone
14. Mackenzie, Anne I.; Barnes, Kevin N.; Nguyen, Truong X., and Scherner, Michael J., "Simulated Versus Measured UHF Radiated Power at LaRC Street Level," NASA/TM-20210013542, April 2021.
15. Butler, Howard; Daly, Martin; Doyle, Allan; Gillies, Sean; Hagen, Stefan; and Schaub, Tim, *Internet Engineering Task Force* Request for Comments (RFC) 7946, ISSN:2070-1721, August 2016.
16. RFD900x and RFD868x Radio Modem Datasheet, *RF Design*, Last Updated December 17, 2020. https://rfdesign.com.au/modems/
17. Alani, Mohammed M., *Guide to Open Systems Interconnection (OSI) and Transmission Control Protocol/Internet Protocol (TCP/IP) Models,* ISBN: 978-3-319-05152-9, Springer, 2014.

*18.* Wetteroth, Debbra*, OSI Reference Model for Telecommunications*, ISBN: 0-07-138041-8, McGraw-Hill, 2002.

*19.* Mackenzie, Anne I., "Simulation of Radio Frequency Power Received by a UAV Along Its Flight Path," NASA/TM-20210020364, August 2021.

20. Winters, Haylee, "RF Environment Data Analysis for UAS Operations," NASA/TM-20220012123, August 2023.

21. Quach, Cuong; Nguyen, Truong; Smalling, Kyle; Rhymer, Nicholas; Mackenzie, Anne; and Santiago, Yamira, "Monitoring Spectrum Occupancy to Assess Communication Link Health for UAS Flight Operations," Unpublished NASA TM, manuscript in preparation, 2025.

22. "What Is OSI Model | Real World Examples," OSI Explainer YouTube

*23.* Nguyen, Truong, "High-Intensity Radiated Field (HIRF) Map - An Avoidance Approach for UAM, AAM, and UAS Vehicles," *Digital Avionics Systems Conf*., October 2023.

*24.* Nguyen, Truong, "HIRF Tolerance and Avoidance for Advanced Air Mobility Vehicles," *Digital Avionics Systems Conf*., October 2024.